To the Graduate Council:

I am submitting herewith a dissertation written by K. Frank Lin entitled "Detailed Analysis of the Calibration of Spectra; An Analysis of $\nu_9 + \nu_{12}$ of C_2H_6." I recommend that it be accepted in partial fulfillment of the requirements for the degree of Doctor of Philosophy, with a major in Physics.

William E. Blass

William E. Blass, Major Professor

We have read this dissertation
and recommend its acceptance:

Robert J. Lovell

Norman M Gailar

Harry C. Jackson

William H. Fletcher

Accepted for the Council:

L Evans Roth

Vice Chancellor
Graduate Studies and Research

DETAILED ANALYSIS OF THE CALIBRATION OF SPECTRA; AN ANALYSIS OF $\nu_9 + \nu_{12}$ OF C_2H_6

A Dissertation

Presented for the

Doctor of Philosophy

Degree

The University of Tennessee, Knoxville

K. Frank Lin

March 1977

ACKNOWLEDGMENTS

I wish to express my appreciation to Dr. William E. Blass who directed this work and provided many innovative suggestions.

I would like to thank Dr. Donald E. Jennings and Dr. Steve Daunt for many stimulating discussions. I would also like to thank a fellow graduate student, Mr. George W. Halsey, for his quick answers to many questions in computer programming.

I wish also to thank Dr. Norman M. Gailar who initiated the design and construction of the spectrometer. I also wish to thank the staff of the University of Tennessee Molecular Spectroscopy Laboratory who designed, built, and maintained many components of the system.

I am deeply indebted to my wife for her assistance in data tabulation and keypunching.

This work was supported by NASA Grant NGL 43-001-006.

ABSTRACT

The first part of this work is a detailed analysis of the calibration of spectra by inserting standard calibration lines in the spectra at regular intervals. The two major types of error, the measurement error and the interpolation error, are examined. The concept of the proper density of the calibration lines is introduced. Seven scans of CO spectra are used to examine the reproducibility and the proper density of the calibration lines of the 5-meter spectrometer. In addition, a comparison is made of two different methods to handle data of several repeated scans.

In the second part of this work the $\nu_9 + \nu_{12}$ band of C_2H_6 near 2024 cm^{-1} is recorded using the 5-meter Littrow instrument. The resolution of the spectra is about 0.020 cm^{-1}. Both the E_u and A_{2u} components of the $E_u \times E_g$ type vibration are observed. Ground state combination differences have been calculated and the ground state molecular parameters B_0, D_0^J, D_0^{JK} are found to be 0.66308141 ($\pm 0.190 \times 10^{-4}$) cm^{-1}, 1.134×10^{-6} ($\pm 0.272 \times 10^{-7}$) cm^{-1}, and 2.396×10^{-6} ($\pm 0.427 \times 10^{-6}$) cm^{-1}, respectively. Various perturbations are observed but not analyzed.

TABLE OF CONTENTS

CHAPTER		PAGE
INTRODUCTION		1
	PART I: DETAILED ANALYSIS OF THE CALIBRATION OF SPECTRA	
I.	THE CALIBRATION OF SPECTRA	4
	Grating Equation	4
	Spectra Recording Methods	5
	Calibration Procedures	5
	Some Comments	7
II.	ERROR ANALYSIS	8
	Error in the Calibration of Spectra	8
	Measurement Error	9
	Interpolation Error	11
	The Proper Density of the Calibration Lines	13
III.	THE ANALYSIS OF A SPECTROMETRIC SYSTEM	16
	Description of the Spectra	16
	Reproducibility of the Displacement of Two Neighboring Lines	19
	Disturbance During the Scanning of Spectra and Irregularity of the Screw	29
	Calculation of the Average Line Positions	29
	Rescaled Average Line Positions	35
	CO 1←0 Band	36
	Determination of the Proper Density of the Calibration Lines	41
	Conclusions	42
	PART II: AN ANALYSIS OF $\nu_9 + \nu_{12}$, C_2H_6	
IV.	VIBRATION-ROTATION THEORY FOR MOLECULES WITH THREEFOLD AXIAL SYMMETRY	44
	The Classical Kinetic Energy	44
	Quantum-Mechanical Hamiltonian	46
	Vibration-Rotation through Fourth Order	48
	Resonances	50

CHAPTER PAGE

Molecular Symmetry Group and Classification of Energy Levels for Symmetric-Top Molecules 50
Selection Rules 51
Intensities of Transitions 52
Transition Frequencies 54
Ground State Combination Differences 56

V. THE $\nu_9 + \nu_{12}$ BAND OF C_2H_6 58

Background 58
Experiment 59
Calibration 59
Measurement and Weighting 60
Assignment 60
Ground State Parameters from Measured Combination Differences 61
Molecular Parameters for the Perpendicular Band of $\nu_9 + \nu_{12}$ 61
Perturbations 74
Conclusions 76

REFERENCES 79

APPENDIXES 83

A. REPRODUCIBILITY OF THE LINE POSITIONS 84
B. APPLICATION OF THE AVERAGE LINE POSITIONS IN THE CALIBRATION OF SPECTRA 87

VITA 90

LIST OF TABLES

TABLE PAGE

PART I

III.1. Assignments and Wavenumbers for the Spectra Containing CO 1←0 and 2←0 Bands 17

III.2. Measured Line Positions of 7 Scans 20

III.3. Displacements between Neighboring Lines 23

III.4. Difference between Displacements of Neighboring Lines and Their Averages 26

III.5. Differences between Line Positions and Average Line Positions 30

III.6. Differences between Rescaled Line Positions and Rescaled Average Line Positions 37

PART II

IV.1. Energy For Axially Symmetric Molecules 49

IV.2. Symmetry Selection Rules for C_{3v} Molecules 53

V.1. Observed $^{Q}R_{K}(J)$ Transitions of $\nu_9 + \nu_{12}$ 64

V.2. Observed $^{Q}P_{K}(J)$ Transitions of $\nu_9 + \nu_{12}$ 65

V.3. Observed $^{P}Q_{K}(J)$ Transitions of $\nu_9 + \nu_{12}$ 66

V.4. Observed $^{P}P_{K}(J)$ Transitions of $\nu_9 + \nu_{12}$ 67

V.5. Observed $^{R}Q_{K}(J)$ Transitions of $\nu_9 + \nu_{12}$ 68

V.6. Observed $^{R}R_{K}(J)$ Transitions of $\nu_9 + \nu_{12}$ 70

V.7. Ground State Parameters for C_2H_6 72

V.8. Results of Previous Studies 73

V.9. Molecule Parameters for the E_u Band of $\nu_9 + \nu_{12}$ 75

LIST OF FIGURES

FIGURE		PAGE
V.1.	Spectra of C_2H_6 from 2018 to 2029 cm^{-1}	62
V.2.	Spectra of C_2H_6 from 2069 to 2090 cm^{-1}	63
V.3.	(Observed Wavenumbers) — (Calculated Wavenumbers) for $^{P}P_{K}(J)$	77
V.4.	(Observed Wavenumbers) — (Calculated Wavenumbers) for $^{R}R_{o}(J)$ and $^{R}Q_{o}(J)$	78

INTRODUCTION

The success of many investigations in infrared spectroscopy depends upon accurate measurements of the wavenumber of infrared lines. Many techniques are currently used for determining the wavenumbers of spectral lines. All of these require wavenumber standards and calibration techniques suitable for the given spectrometer.

In attempting to attain high precision in the wavenumber determination of spectral lines, it is important to understand the possible sources of error and to determine the reliability of the calibration technique. In Part I of this study the expressions for the two major sources of error, the measurement error and the interpolation error are obtained. The performance of a screw-driven tangent arm scanning instrument which samples data at equal time increments under "clock" control is investigated. Most of the procedures used are general enough to be applied to other types of data taking systems as long as only one dependent variable and one independent variable are involved. The results of these investigations enhance our confidence in the calculated wavenumbers for the unknown spectral lines.

When a sufficient number of calibration lines are present in the spectra, the standard deviation of the measured wavenumbers obtained by averaging the results of 3 (7) scans for 22 CO 1←0 lines is found to be 0.00095 cm^{-1} (0.00063 cm^{-1}). The accuracy of a measured wavenumber is 1 part in 2.2×10^6 (3.3×10^6) for 3 (7) scans.

Part II of this study describes an analysis of a combination band of ethane, $\nu_9 + \nu_{12}$.

For the combination band $\nu_9 + \nu_{12}$, both the A_{2u} and E_u bands of the $E_u \times E_g$ type vibration are observed. The perpendicular band is centered at 2024 cm^{-1} and the parallel band at 2008 cm^{-1}. Approximately 700 transitions are assigned in the perpendicular band and 300 transitions assigned in the parallel band. About 410 properly weighted ground state combination differences (GSCD) are used to obtain the ground state parameters B_0, D_0^J, D_0^{JK}. The results are $B_0 = 0.66308140$ ($\pm 0.19 \times 10^{-4}$) cm^{-1}, $D_0^J = 1.134 \times 10^{-6}$ ($\pm 0.272 \times 10^{-7}$) cm^{-1}, $D_0^{JK} = 2.396 \times 10^{-6}$ ($\pm 0.427 \times 10^{-6}$) cm^{-1}. Besides the ℓ-type doubling in the K = 0 subband, the perpendicular band is perturbed in the subbands with K K = -1 to -7. The parallel band is also perturbed; no satisfactory explanation for these perturbations has been found.

PART I

DETAILED ANALYSIS OF THE CALIBRATION OF SPECTRA

CHAPTER I

THE CALIBRATION OF SPECTRA

The wavenumbers of the spectral lines in a spectrum are determined through calibration procedures. Very often it is desired to be able to determine the wavenumbers as accurate as possible; the calibration of spectra should be accomplished carefully and properly. In this chapter the background of the calibration process in grating spectroscopy is briefly described.

I.A. GRATING EQUATION

The grating equation for a Littrow spectrometer can be expressed in the form

$$\nu = nk \csc \theta \tag{1.1}$$

where n is the spectral order, k is the instrument constant (expressed in cm^{-1}) and θ is the angle between the central image and the spectral line located at ν cm^{-1}. In this case the exit and entrance slits are assumed to be coincident.

When this is not the case, the grating equation has to be derived from the particular design of the optical system. For the University of Tennessee Molecular Spectroscopy Laboratory (UTMSL) 5-meter Littrow Spectrometric System, the grating equation can be written as

$$\nu = nk \sec \delta \csc \theta \tag{1.2}$$

where 2δ is the angle between the entrance and exit slits as seen from the collimator (1).

If $k \sec \delta$ is written as k' then Eq. (1.2) can be written as

$$\nu = nk' \csc \theta \tag{1.3}$$

which is exactly the same form as Eq. (1.1).

I.B. SPECTRA RECORDING METHODS

The scanning of a spectrum is usually accomplished by rotating the grating. In many installations spectra are recorded using an analog strip chart recorder. With the development of modern digital techniques, more and more spectra are recorded digitally. In most cases, no matter how the spectra are recorded, $\frac{\Delta\theta}{\Delta x}$ is intended to be a constant, where $\Delta\theta$ is a small increment of the grating angle and Δx is the corresponding small increment of the data recording parameter. For the chart recording system x will be the position on the chart paper. For digital recording system x will be the index for the sequentially sampled data, which is usually referred to as data point number. For digitalized data the value of Δx will be set equal to 1.

I.C. CALIBRATION PROCEDURES

If $\frac{\Delta\theta}{\Delta x}$ can really be kept constant during a scan, then the calibration of the spectra will be very simple. But due to the limitation incurred by the quality of the grating scanning devices, the value of $\frac{\Delta\theta}{\Delta x}$ will vary slightly during a scan.

The variation of $\frac{\Delta\theta}{\Delta x}$ can be time-dependent as well as time-independent. If the variation is time-dependent, then it is possible to calibrate the instrument. Otherwise the relation between θ and x, written as $\theta(x)$, must be determined for every scan of the spectra.

In a spectrum if a set of angles, $\{\theta_1,\theta_2, \ldots , \theta_n\}$, is known to correspond to a set of x-values, $\{x_1,x_3, \ldots , x_n\}$, then an interpolation function can be determined to calculate the angles and therefore the wavenumbers for the spectral lines in the range of interpolation. Usually the known values for the set of paired observations $\{(\theta_1,x_1), (\theta_2,x_2), \ldots , (\theta_n,x_n)\}$, are obtained by recording well-known spectral lines, which are called calibration lines, in or along with the spectra at regular wavenumber intervals (2). For convenience the measured x-value for a spectral line will be called the line position.

Let $\theta(x)$ denote the real and usually known function that relates the grating angle θ and data recording parameter x; then the grating equation can be written as

$$\nu = nk \csc \theta(x) . \tag{1.4}$$

A polynomial in the form

$$\nu = \sum_{i=0}^{n} a_i x^i \tag{1.5}$$

can be used as a proper approximation of Eq. (1.4) if n is properly chosen. Very often Eq. (1.5) is used as a model function in an equation-fitting procedure.

The techniques of fitting equations to data are well presented in many books such as Draper and Smith (3) and Daniel and Wood (4). In this presentation it will be assumed that the calibration equations are properly obtained by the available data fitting techniques.

I.D. SOME COMMENTS

To determine the wavenumbers of the spectral lines, the function that is desired is $\nu(x)$. $\nu(x)$ can be determined without knowing the form of the grating equation. However, it is more convenient to examine the sources of error and the reliability of the calibration procedures in terms of θ and x. So the determination of $\theta(x)$ will be discussed.

Theoretically, for the paired observations, $\{(\theta_i, x_i)'s\}$, the variable that is known more accurately should be taken as the independent variable and the other as the dependent variable in an equation-fitting procedure. In infrared studies the wavenumbers of the calibration lines usually are better known than the line positions. Accordingly, θ should be considered as the independent variable and x as the dependent variable. But $\theta(x)$ is more desirable than $x(\theta)$. So it will be assumed the same relation between θ and x will be obtained no matter which variable is considered as the independent variable.

CHAPTER II

ERROR ANALYSIS

The error in the calibration of spectra will be examined in this chapter. Although the overlapping of the neighboring spectral lines is a major source of error, it is excluded from the following discussion.

II.A. ERROR IN THE CALIBRATION OF SPECTRA

If the spectral lines are well separated from each other, then the error of the calculated grating angle for a spectral line at line position x_i by a calibration function can be considered due to the combination of the following two types of error:

1. Error in the measured line position. (This will be referred to as the measurement error and denoted by ε_i.)
2. Error in the calibration function. (This will be referred to as the interpolation error.)

The noise that is present with the signal has long been recognized as the cause of the measurement error. The interpolation error is due to the insufficiency of data to determine $\theta(x)$. Both types of error will be further examined in the following sections.

Let $\hat{\theta}(x)$ denote the determined function which estimates $\theta(x)$. Then the error of the determined grating angle for a spectral line at line position x_i can be written as

$$R = [\hat{\theta}(x_i) - \theta(x_i)] + \left.\frac{\Delta\hat{\theta}}{\Delta x}\right|_{x_i} \cdot \varepsilon_i \ . \qquad (2.1)$$

From this expression it is easily observed that even if $\theta(x)$ is determined exactly, i.e., $\hat{\theta}(x) = \theta(x)$, R will be equal to $\left.\frac{\Delta\hat{\theta}}{\Delta x}\right|_{x_i} \cdot \varepsilon_i$, which usually is nonzero. This implies that if the variance of $\hat{\theta}(x) - \theta(x)$, which is defined to be the average value of $(\hat{\theta}(x) - \theta(x))^2$, is much less than the variance of $\frac{d\theta}{dx} \cdot \varepsilon_i$, the calibration of spectra cannot be significantly improved unless noise level is reduced. This is important to bear in mind.

II.B. MEASUREMENT ERROR

Since all the spectral lines are of finite width, the apparent line positions are affected by the noise present with the signal. If the distribution function for the noise is known, then theoretically, the distribution function for the measurement error can be obtained. It is useful to obtain an expression for the variance of the distribution function for the measurement error in terms of related physical quantities.

For the convenience of discussion, it will be assumed that the spectra are digitally sampled at equal grating angle intervals Δ, and the noise at each data point is gaussian and independent of each other. Let the full width at half height (FWHH) of a spectral line be denoted by F. The value for F/Δ will be assumed to be large enough (≥ 50) that it is sufficient to determine the line center by the index of the data points. Let G(i) and N(i) denote the signal and the noise at data point i and let M be a chosen number which satisfies the relation $M \cdot \Delta \leq F$. Considering the symmetric profile of a spectral line, the line center will be assumed to be at $x = n_i$, if

$$C(n_i) = \left| \sum_{i=n_i-M}^{n_i-1} (G(i) + N(i)) - \sum_{i=n_i+1}^{n_i+M} (G(i) + N(i)) \right| \qquad (2.2)$$

is a local minimum.

Let x_i denote the center position of the noise-free spectral line, then the variance of the measurement error is the variance of $n_i - x_i$. Let

$$A_1 = \sum_{i=x_i-M}^{x_i-1} N(i) \qquad (2.3)$$

and

$$A_2 = \sum_{i=x_i+1}^{x_i+M} N(i) \qquad (2.4)$$

then to the first order of approximation

$$n_i - x_i = (A_2 - A_1)/2(G(n_i) - G(n_i - M)) \; . \qquad (2.5)$$

Since the noise at each data point is independent of each other, the distribution function for A_1 and A_2 can be assumed to be gaussian

$$f(A) = \frac{1}{\sqrt{\pi}a} e^{-\frac{A^2}{a^2}} \; . \qquad (2.6)$$

From "random walk theory" (5,6) the value for a is

$a = \sqrt{M} \cdot \hat{N}$ ($\hat{N}$ is the root-mean-square value of the noise).

The variance of $n_i - x_i$ can be written as

$$\overline{(n_i - x_i)^2} = \int_{-\infty}^{\infty} \int_{-\infty}^{\infty} \left[\frac{A_2 - A_1}{2(G(n_i) - G(n_i - M))}\right]^2 \cdot f(A_1) \cdot f(A_2) dA_1 \, dA_2 \, . \tag{2.5}$$

The integration on the right hand side can be shown to be equal to $\frac{a^2}{4[G(n_i)-G(n_i-M)]^2}$. If M is set equal to F/2 , which means the line center is measured using the absorption profile within FWHM only, then the expression for $(\overline{(n_i-x_i)^2})^{1/2}$ is

$$(\overline{(n_i-x_i)^2})^{1/2} = \frac{\frac{\overline{F}}{2} \cdot \hat{N}}{G(n_i)} \, . \tag{2.6}$$

Equation (2.6) can be used to estimate the measurement error if $\frac{\Delta\theta}{\Delta x}$ is roughly known, where Δx is a small increment of the data point number and $\Delta\theta$ is the corresponding increment of the grating angle.

It is possible to determine the center position of a spectral line by other criteria, but the variance of the measurement error is expected to be about the same.

II.C. INTERPOLATION ERROR

The function $\theta(x)$ is usually obtained by fitting a proposed model equation to the paired numbers, $\{(\theta_1,x_1), (\theta_2,x_2), \ldots , (\theta_n,x_n)\}$, where θ_i, x_i is the grating angle and line position for the ith calibration line. The measured values for x_i's will include measurement error too. For convenience of discussion, the measurement error for x_i's will be assumed to be zero in this section.

Because of the variation of $\frac{\Delta\theta}{\Delta x}$, even if the measurement error for x's vanishes $\theta(x)$ cannot be determined exactly. The variance of $\hat{\theta}(x) - \theta(x)$ depends on the characteristic of the variation of $\frac{\Delta\theta}{\Delta x}$ and usually is difficult to evaluate.

If $\hat{\theta}$ is determined with $\hat{\theta}(x_i) = \theta_i$ and $\frac{\Delta\theta}{\Delta x} - \frac{\Delta\theta}{\Delta x}$ is assumed to be random and gaussian, then $\frac{\Delta\theta}{\Delta x}$ can be written as

$$\frac{\Delta\theta}{\Delta x} = \frac{\Delta\hat{\theta}}{\Delta x} + S(x) \tag{2.7}$$

where $S(x)$ represents the fluctuational part of $\frac{\Delta\theta}{\Delta x}$. Because

$$\sum_{x=x1}^{x_{i+1}} \frac{\Delta\hat{\theta}(x)}{\Delta x} = \theta_{i+1} - \theta_i,$$

$S(x)$ must satisfy the relation

$$\sum_{x=x_i}^{x_{i+1}} S(x) = 0 .$$

Let the distribution function of S be expressed by

$$W(S) = \frac{1}{\sqrt{\pi}a} e^{-\frac{s^2}{a^2}},$$

then the average dispersion of $\hat{\theta}(x) - \theta(x)$ between x_i and x_{i+1}, the data point values for calibration lines at θ_i and θ_{i+1}, are proportional to

$$D = \frac{1}{(x_{i+1}-x_i+1)} \iint \cdots \int \sum_{k=x_i}^{x_{i+1}} \Big(\sum_{x=x_i}^{k} S(x_i) \Big)^2 W(S(x_i))$$

$$\cdot\, W(S(x_i+1)) \cdots W(S(x_{i+1})) \cdot \delta\Big(\sum_{x=x_i}^{x_{i+1}} S(x)\, dS(x_i) dS(x_i+1) \cdots dS(x_{i+1}) \Big). \tag{2.8}$$

Using the relation $\delta(\sum_x S(x)) = \frac{1}{2\pi} \int dk\, e^{-ik(\sum_x S(x))}$, D is found to be

$$\frac{a}{12\sqrt{\pi}} \cdot \frac{(x_{i+1}-x_i)(x_{i+1}-x_i+z)}{(x_{i+1}-x_i+1)} \cdot \frac{1}{\sqrt{x_{i+1}-x_i+1}},$$

which is approximately equal to $\frac{a}{12\sqrt{\pi}} \cdot \sqrt{x_{i+1}-x_i}$. From this expression for D it is easily observed that the interpolation error decreases as the distance between two neighboring calibration lines is decreased.

Now it can be easily observed that the interpolation error can be rendered as small as desired if the density of the calibration lines can be chosen at will. In practice the density of calibration lines is limited.

II.D. THE PROPER DENSITY OF THE CALIBRATION LINES

In the discussion in Section II.C, it is assumed that the measurement error for the calibration lines vanishes. This assumption is usually not true in practice. When a calibration algorithm is used to obtain a calibration equation for a spectrum, the variance of the calibration fit is naturally due to both types of error.

In the following discussion it will be assumed that the variance of the calibration fit is about the same as the variance of the calculated grating angles for the spectral lines of interest if the measurement error is about the same for all the spectral lines.

Since the variance of the calculated grating angle for a spectral line of interest is due to the combination of the variance of the measurement error and the variance of the interpolation error, there is no practical need to make the contribution of the latter less than 25% of that of the former.

For a particular spectrum, if the density of the calibration lines can be chosen at will, then for some density of the calibration lines the contribution of the interpolation error can be rendered approximately equal to 25% of that of the measurement error. As far as accuracy is concerned, there is no practical need to insert much more calibration lines in the spectra, so such density of calibration lines will be called the proper density of the calibration lines.

Let $\hat{\theta}_1$ and $\hat{\theta}_2$ be two calibration equations for the same spectrum using substantially different densities of calibration lines. (A ratio of 2 to 1 can be considered substantially different.) If the variances of these two fits are about equal and the variance of $\hat{\theta}_1(x) - \hat{\theta}_2(s)$ is about equal to 20% of the variance of the fits, it is quite safe to assume the variance of $\hat{\theta}_i(x) - \hat{\theta}(x)$, i = 1 or 2, will be less than 20% of the variance of the fits. (If the fits are properly obtained, the variance of $\hat{\theta}_i(x) - \theta(x)$ should be $\simeq$ the variance of $\hat{\theta}_1(x) - \hat{\theta}_2(x)$.)

If a model equation for $\nu(x)$ is used in the calibration fit, the concept of the proper density of the calibration lines and the procedure to determine it also seems to be applicable.

CHAPTER III

THE ANALYSIS OF A SPECTROMETRIC SYSTEM

It is important to determine the stability and reproducibility of the scanning mechanism of a spectrometer since this in turn determines the calibration procedures needed for reliable measurements. In this chapter the performance of the 5-meter Littrow spectrometer is closely examined. Some observed phenomena are explained and the proper density of the calibration lines is determined.

III.A. DESCRIPTION OF THE SPECTRA

Consider the data of seven scans of CO 1←0 and 2←0 bands, which are taken with a Bausch and Lomb 20 cm x 41 cm grating with 31.6 grooves per millimeter. The grating is set to rotate continuously at constant speed, and the prism is controlled by the computer to switch between 12th and 24th (or 25th) orders to permit the lines of the 2←0 and 1←0 bands to be observed. The pressure of CO is 3 torr and the path-length of the sample cell is 4 meters. Twenty-seven lines of the 1←0 band and forty-eight lines of the 2←0 band are observed in the spectra. Due to various problems in some scans, the number of measured line positions varies slightly from scan to scan. A common index is used to label the spectral lines according to the order of the appearance of the lines on the spectra.

The assignments and the wavenumbers of the lines in the CO spectra are listed in Table III.1. The wavenumbers used are determined by

TABLE III.1

ASSIGNMENTS AND WAVENUMBERS FOR THE SPECTRA
CONTAINING CO 1←0 AND 2←0 BANDS

	Assignments		
	1←0	2←0	Wavenumbers
1	P22		2050.85452
2	P21		2055.40077
3		R6	4285.0093
4		R7	4288.2901
5		R8	4291.4998
6		R9	4294.6381
7		R10	4297.7050
8	P19		2064.39734
9		R12	4303.6236
10		R13	4306.4752
11		R14	4309.]547
12	P18		2068.84737
13		R15	4311.9619
14		R16	4314.5968
15		R17	4317.1593
16	P17		2073.26504
17		R19	4322.0660
18		R20	4324.4100
19		R21	4326.6810
20	P16		2077.65019
21	P15		2082.00269
22	P14		2086.32238
23		P19	4175.2027
24		P18	4180.2828
25	P13		2090.60913
26		P17	4185.2955
27	P12		2094.86278
28		P16	4190.2407
29		P15	4195.1182
30	P11		2099.08318
31		P14	4199.9280
32		P13	4204.6698
33	P10		2103.27019
34		P12	4209.3435
35		P11	4213.9489
36	P9		2107.42367
37		P10	4218.4860
38	P8		2111.54346

TABLE III.1 (continued)

	Assignments		
	1←0	2←0	Wavenumbers
39		P8	4227.3544
40	P7		2115.62942
41		P7	4231.6853
42		P6	4235.9474
43	P6		2119.68140
44		P5	4240.1402
45		P4	4244.2639
46	P5		2123.69926
47		P3	4248.3180
48	P4		2127.68285
49		P1	4256.2176
50	P3		2131.63202
51		R0	4263.8376
52		R1	4267.5425
53	P2		2135.54663
54		R3	4274.7411
55		R4	4278.2347
56	P1		2139.42652
57		R5	4281.6574
58		R6	4285.0093
59		R7	4288.2901
60		R8	4291.4998
61	R0		2147.08158
62		R10	4297.7050
63		R11	4300.7002
64	R1		2150.85645
65		R12	4303.6236
66		R13	4306.4752
67	R2		2154.59603
68		R15	4311.9619
69		R16	4314.5968
70	R3		2158.30016
71		R17	4317.1593
72		R18	4319.6490
73		R19	4322.0660
74	R5		2165.60149
75	R6		2169.19840

Guelachvili (7,8). The measured line positions are listed in Table III.2. The missing lines in a particular scan are recorded as X = 0. The measured ith line position in the jth scan will be denoted as X_{ij}.

III.B. REPRODUCIBILITY OF THE DISPLACEMENT OF TWO NEIGHBORING LINES

For two neighboring lines in the jth scan the distance between them will be defined by $d_{ij} = X_{ij} - X_{i-1,j}$. A comparison of all the values of the displacements for two neighboring lines will indicate the consistency and reproducibility of our scanning device in a short range. All the available values of d_{ij}'s are listed in Table III.3. Column 8 of Table III.3 lists the averaged values of the distance of neighboring lines, which will be denoted by $\bar{d}_i$. The averages are obtained by two steps. In the first step, all the values of the d_{ij}'s for some i are used to get the average distances. In the second step, those d_{ij}'s that deviate from their average distances by more than 0.3% of the average distance are deleted. Then a new set of average distances, which will be called filtered average distance, is obtained by excluding those deleted values. The differences between the d_{ij}'s and their corresponding averaged distances are listed in Table III.4.

The fact that only about 5% of the d_{ij}'s are deleted indicates the scan mechanism can reproduce the distance between neighboring lines within 0.3% with about 95% level of confidence.

TABLE III.2

MEASURED LINE POSITIONS OF 7 SCANS

	(1)	(2)	(3)	(4)	(5)	(6)	(7)
1	0.0	0.0	0.0	0.0	0.0	0.0	0.0
2	9423.0	9428.0	9442.0	9474.0	9418.0	9492.0	9443.0
3	12296.0	12310.0	0.0	12360.0	0.0	12376.0	12330.0
4	15515.0	15517.0	15545.0	15581.0	15510.0	15591.0	15544.0
5	18638.0	18640.0	18660.0	18715.0	18631.0	18716.0	18675.0
6	21680.0	21683.0	21718.0	21761.0	21670.0	21757.0	21717.0
7	24628.0	24635.0	24673.0	24716.0	24620.0	24714.0	24667.0
8	27616.0	27622.0	27668.0	27711.0	27602.0	27704.0	27653.0
9	30280.0	30287.0	30345.0	30390.0	30273.0	30376.0	30324.0
10	32987.0	32988.0	33057.0	33098.0	32976.0	33083.0	33030.0
11	35611.0	35609.0	35687.0	35731.0	35597.0	35705.0	35653.0
12	36404.0	36401.0	36474.0	36526.0	36385.0	36499.0	36442.0
13	38153.0	38152.0	38239.0	38281.0	38135.0	38255.0	38195.0
14	40615.0	40616.0	40708.0	40755.0	40596.0	40721.0	40659.0
15	42999.0	43004.0	43100.0	43146.0	42982.0	43107.0	43041.0
16	44985.0	44985.0	45090.0	45137.0	44962.0	0.0	45026.0
17	47541.0	47539.0	47652.0	47717.0	47518.0	47654.0	47582.0
18	49700.0	49701.0	0.0	49877.0	49675.0	49810.0	49740.0
19	51782.0	51776.0	0.0	51964.0	51755.0	51898.0	51821.0
20	53379.0	53382.0	53556.0	53561.0	53350.0	53495.0	53418.0
21	61586.0	61590.0	61776.0	61784.0	61550.0	61712.0	61622.0
22	69616.0	69621.0	69819.0	69824.0	69577.0	69745.0	69651.0
23	71975.0	71984.0	72188.0	72188.0	71935.0	72105.0	72010.0
24	76617.0	76635.0	76843.0	76845.0	76581.0	76756.0	76659.0
25	77468.0	77480.0	77693.0	77694.0	77428.0	77602.0	77505.0
26	81170.0	81185.0	81400.0	81401.0	81131.0	81306.0	81207.0
27	85156.0	85177.0	85396.0	85393.0	85117.0	85293.0	85192.0
28	85629.0	85641.0	85864.0	85861.0	85586.0	85762.0	85659.0
29	89984.0	90003.0	90226.0	90224.0	89944.0	90123.0	90020.0

TABLE III.2 (continued)

	(1)	(2)	(3)	(4)	(5)	(6)	(7)
30	92685.0	92709.0	92939.0	92932.0	92645.0	92826.0	92723.0
31	94246.0	94270.0	94502.0	94498.0	94209.0	94390.0	94286.0
32	98419.0	98446.0	98682.0	98676.0	98380.0	98563.0	98459.0
33	100055.0	100082.0	100332.0	100317.0	0.0	100197.0	100093.0
34	102504.0	102532.0	102775.0	102770.0	102468.0	102650.0	102543.0
35	106501.0	106531.0	106774.0	106770.0	106465.0	106649.0	106545.0
36	107274.0	107304.0	107547.0	107542.0	107235.0	107421.0	107316.0
37	110412.0	110442.0	110692.0	110684.0	110374.0	110557.0	110454.0
38	114344.0	114381.0	114635.0	114623.0	114309.0	114492.0	114388.0
39	117977.0	118014.0	118275.0	118265.0	117937.0	118128.0	118021.0
40	121274.0	121313.0	121576.0	121566.0	121235.0	121427.0	121320.0
41	0.0	0.0	121943.0	121929.0	0.0	121790.0	121683.0
42	125217.0	125258.0	125530.0	125515.0	125174.0	125369.0	125261.0
43	128065.0	128109.0	128380.0	128368.0	128017.0	128220.0	128111.0
44	128719.0	128761.0	129035.0	129019.0	128674.0	128873.0	128763.0
45	132138.0	132186.0	132462.0	132446.0	132095.0	132297.0	132187.0
46	134722.0	134771.0	135053.0	135036.0	134680.0	134883.0	134772.0
47	135484.0	135533.0	135813.0	135799.0	135440.0	135645.0	135533.0
48	141243.0	141293.0	141582.0	141568.0	141205.0	141409.0	141295.0
49	0.0	141999.0	142287.0	142272.0	141910.0	142113.0	142000.0
50	147649.0	147704.0	147995.0	147983.0	147615.0	147820.0	147704.0
51	0.0	148173.0	148463.0	148449.0	148084.0	148288.0	148174.0
52	151093.0	151151.0	151443.0	151431.0	151065.0	151266.0	151153.0
53	153927.0	153986.0	154279.0	154269.0	153900.0	154102.0	153988.0
54	156835.0	156894.0	157190.0	157177.0	156812.0	157013.0	156894.0
55	159607.0	159663.0	159958.0	159947.0	159581.0	159785.0	159665.0
56	160093.0	160145.0	160443.0	160434.0	160064.0	160267.0	160149.0
57	162306.0	162365.0	162663.0	162650.0	162281.0	162485.0	162368.0
58	164937.0	164996.0	165294.0	165283.0	164917.0	165118.0	165000.0
59	167505.0	167564.0	167861.0	167853.0	167484.0	167683.0	167569.0
60	170003.0	170062.0	170357.0	170347.0	169982.0	170181.0	170066.0

TABLE III.2 (continued)

	(1)	(2)	(3)	(4)	(5)	(6)	(7)
61	172063.0	172124.0	172423.0	172411.0	172045.0	172246.0	172129.0
62	174803.0	174864.0	175166.0	175154.0	174786.0	174989.0	174870.0
63	177109.0	177169.0	177466.0	177454.0	177091.0	177292.0	177173.0
64	177882.0	177943.0	178244.0	178231.0	177863.0	178065.0	177946.0
65	179345.0	179407.0	179705.0	179696.0	179328.0	179531.0	179412.0
66	181521.0	181578.0	181889.0	181876.0	181505.0	181707.0	181587.0
67	183582.0	0.0	183954.0	0.0	183564.0	183768.0	183648.0
68	185687.0	185745.0	186062.0	0.0	185667.0	185870.0	185752.0
69	187672.0	187739.0	188047.0	0.0	187660.0	187859.0	187741.0
70	189184.0	0.0	189556.0	0.0	189168.0	189371.0	189250.0
71	0.0	189671.0	189986.0	0.0	0.0	0.0	189678.0
72	191465.0	191533.0	191845.0	0.0	191462.0	191666.0	191545.0
73	0.0	0.0	193651.0	0.0	193269.0	193472.0	193358.0
74	200061.0	0.0	200456.0	0.0	200051.0	200249.0	200134.0
75	205352.0	0.0	205750.0	0.0	205344.0	205544.0	205426.0

TABLE III.3

DISPLACEMENTS BETWEEN NEIGHBORING LINES

	(1)	(2)	(3)	(4)	(5)	(6)	(7)	Average
1	0.0	0.0	0.0	0.0	0.0	0.0	0.0	0.0
2	9423.0	9428.0	9442.0	9474.0	9418.0	9492.0	9443.0	9445.7
3	2873.0	2882.0	0.0	2886.0	0.0	2884.0	2887.0	2882.4
4	3219.0	3207.0	0.0	3221.0	0.0	3215.0	3214.0	3215.2
5	3123.0	3123.0	3115.0	3134.0	3121.0	3125.0	3131.0	3124.6
6	3042.0	3043.0	3058.0	3046.0	3039.0	3041.0	3042.0	3044.4
7	2948.0	2952.0	2955.0	2955.0	2950.0	2957.0	2950.0	2952.4
8	2988.0	2987.0	2995.0	2995.0	2982.0	2990.0	2986.0	2989.0
9	2664.0	2665.0	2677.0	2679.0	2671.0	2672.0	2671.0	2671.3
10	2707.0	2701.0	2712.0	2708.0	2703.0	2707.0	2706.0	2706.3
11	2624.0	2621.0	2630.0	2633.0	2621.0	2622.0	2623.0	2624.9
12	793.0	792.0	787.0	795.0	788.0	794.0	789.0	791.1
13	1749.0	1751.0	1765.0	1755.0	1750.0	1756.0	1753.0	1754.1
14	2462.0	2464.0	2469.0	2474.0	2461.0	2466.0	2464.0	2465.7
15	2384.0	2388.0	2392.0	2391.0	2386.0	2386.0	2382.0	2387.0
16	1986.0	1981.0	1990.0	1991.0	1980.0	0.0	1985.0	1985.5
17	2556.0	2554.0	2562.0	2580.0	2556.0	0.0	2556.0	2560.7
18	2159.0	2162.0	0.0	2160.0	2157.0	2156.0	2158.0	2158.7
19	2082.0	2075.0	0.0	2087.0	2080.0	2088.0	2081.0	2082.2
20	1597.0	1606.0	0.0	1597.0	1595.0	1597.0	1597.0	1598.2
21	8207.0	8208.0	8220.0	8223.0	8200.0	8217.0	8204.0	8211.3
22	8030.0	8031.0	8043.0	8040.0	8027.0	8033.0	8029.0	8033.3
23	2359.0	2363.0	2369.0	2364.0	2358.0	2360.0	2359.0	2361.7
24	4642.0	4651.0	4655.0	4657.0	4646.0	4651.0	4649.0	4650.1
25	851.0	845.0	850.0	849.0	847.0	846.0	846.0	847.7
26	3702.0	3705.0	3707.0	3707.0	3703.0	3704.0	3702.0	3704.3
27	3986.0	3992.0	3996.0	3992.0	3986.0	3987.0	3985.0	3989.1
28	473.0	464.0	468.0	468.0	469.0	469.0	467.0	468.3
29	4355.0	4362.0	4362.0	4363.0	4358.0	4361.0	4361.0	4360.3

TABLE III.3 (continued)

	(1)	(2)	(3)	(4)	(5)	(6)	(7)	Average
30	2701.0	2706.0	2713.0	2708.0	2701.0	2703.0	2703.0	2705.0
31	1561.0	1561.0	1563.0	1566.0	1564.0	1564.0	1563.0	1563.1
32	4173.0	4176.0	4180.0	4178.0	4171.0	4173.0	4173.0	4174.9
33	1636.0	1636.0	1650.0	1641.0	0.0	1634.0	1634.0	1638.5
34	2449.0	2450.0	2443.0	2453.0	0.0	2453.0	2450.0	2449.7
35	3997.0	3999.0	3999.0	4000.0	3997.0	3999.0	4002.0	3999.0
36	773.0	773.0	773.0	772.0	770.0	772.0	771.0	772.0
37	3138.0	3138.0	3145.0	3142.0	3139.0	3136.0	3138.0	3139.4
38	3932.0	3939.0	3943.0	3939.0	3935.0	3935.0	3934.0	3936.7
39	3633.0	3633.0	3640.0	3642.0	3628.0	3636.0	3633.0	3635.0
40	3297.0	3299.0	3301.0	3301.0	3298.0	3299.0	3299.0	3299.1
41	0.0	0.0	367.0	363.0	0.0	363.0	363.0	364.0
42	0.0	0.0	3587.0	3586.0	0.0	3579.0	3578.0	3582.5
43	2848.0	2851.0	2850.0	2853.0	2843.0	2851.0	2850.0	2849.4
44	654.0	652.0	655.0	651.0	657.0	653.0	652.0	653.4
45	3419.0	3425.0	3427.0	3427.0	3421.0	3424.0	3424.0	3423.9
46	2584.0	2585.0	2591.0	2590.0	2585.0	2586.0	2585.0	2586.6
47	762.0	762.0	760.0	763.0	760.0	762.0	761.0	761.4
48	5759.0	5760.0	5769.0	5769.0	5765.0	5764.0	5762.0	5764.0
49	0.0	706.0	705.0	704.0	705.0	704.0	705.0	704.8
50	0.0	5705.0	5708.0	5711.0	5705.0	5707.0	5704.0	5706.7
51	0.0	469.0	468.0	466.0	469.0	468.0	470.0	468.3
52	0.0	2978.0	2980.0	2982.0	2981.0	2978.0	2979.0	2979.7
53	2834.0	2835.0	2836.0	2838.0	2835.0	2836.0	2835.0	2835.6
54	2908.0	2908.0	2911.0	2908.0	2912.0	2911.0	2906.0	2909.1
55	2772.0	2769.0	2768.0	2770.0	2769.0	2772.0	2771.0	2770.1
56	486.0	482.0	485.0	487.0	483.0	482.0	484.0	484.1
57	2213.0	2220.0	2220.0	2216.0	2217.0	2218.0	2219.0	2217.6
58	2631.0	2631.0	2631.0	2633.0	2636.0	2633.0	2632.0	2632.4
59	2568.0	2568.0	2567.0	2570.0	2567.0	2565.0	2569.0	2567.7
60	2498.0	2498.0	2496.0	2494.0	2498.0	2498.0	2497.0	2497.0

TABLE III.3 (continued)

	(1)	(2)	(3)	(4)	(5)	(6)	(7)	Average
61	2060.0	2062.0	2066.0	2064.0	2063.0	2065.0	2063.0	2063.3
62	2740.0	2740.0	2743.0	2743.0	2741.0	2743.0	2741.0	2741.6
63	2306.0	2305.0	2300.0	2300.0	2305.0	2303.0	2303.0	2303.1
64	773.0	774.0	778.0	777.0	772.0	773.0	773.0	774.3
65	1463.0	1464.0	1461.0	1465.0	1465.0	1466.0	1466.0	1464.3
66	2176.0	2171.0	2184.0	2180.0	2177.0	2176.0	2175.0	2177.0
67	2061.0	0.0	2065.0	0.0	2059.0	2061.0	2061.0	2061.4
68	2105.0	0.0	2108.0	0.0	2103.0	2102.0	2104.0	2104.4
69	1985.0	1994.0	1985.0	0.0	1993.0	1989.0	1989.0	1989.2
70	1512.0	0.0	1509.0	0.0	1508.0	1512.0	1509.0	1510.0
71	0.0	0.0	430.0	0.0	0.0	0.0	428.0	429.0
72	0.0	1862.0	1859.0	0.0	0.0	0.0	1867.0	1862.7
73	0.0	0.0	1806.0	0.0	1807.0	1806.0	1813.0	1808.0
74	0.0	0.0	6805.0	0.0	6782.0	6777.0	6776.0	6785.0
75	5291.0	0.0	5294.0	0.0	5293.0	5295.0	5292.0	5293.0

TABLE III.4

DIFFERENCE BETWEEN DISPLACEMENTS OF NEIGHBORING LINES AND THEIR AVERAGES

	(1)	(2)	(3)	(4)	(5)	(6)	(7)
1	0.0	0.0	0.0	0.0	0.0		0.0
2	-15.0	-10.0	4.0	36.0	-20.0	54.0	5.0
3	-11.8	-2.8	0.0	1.3	0.0	-0.8	2.3
4	3.4	-8.2	0.0	5.8	0.0	-0.2	-1.2
5	-1.6	-1.6	-9.6	9.4	-3.6	0.4	6.4
6	-0.2	0.8	15.8	3.8	-3.2	-1.2	-0.2
7	-4.4	-0.4	2.6	2.6	-2.4	4.6	-2.4
8	-1.0	-2.0	6.0	6.0	-7.0	1.0	-3.0
9	-7.3	-6.3	5.7	7.7	-0.3	0.7	-0.3
10	0.7	-5.3	5.7	1.7	-3.3	0.7	-0.3
11	0.5	-2.5	6.5	9.5	-2.5	-1.5	-0.5
12	1.7	0.7	-4.3	3.7	-3.3	2.7	-2.3
13	-3.3	-1.3	12.7	2.7	-2.3	3.7	0.7
14	-2.3	-0.3	4.7	9.7	-3.3	1.7	-0.3
15	-3.0	1.0	5.0	4.0	-1.0	-1.0	-5.0
16	0.5	-4.5	4.5	5.5	-5.5	0.0	-0.5
17	-0.8	-2.8	5.2	23.2	-0.8	0.0	-0.8
18	0.3	3.3	0.0	1.3	-1.7	-2.7	-0.7
19	-1.6	-8.6	0.0	3.4	-3.6	4.4	-2.6
20	0.4	9.4	0.0	0.4	-1.6	0.4	0.4
21	-4.3	-3.3	8.7	11.7	-11.3	5.7	-7.3
22	-3.3	-2.3	9.7	6.7	-6.3	-0.3	-4.3
23	-1.5	2.5	8.5	3.5	-2.5	-0.5	-1.5
24	-8.1	0.9	4.9	6.9	-4.1	0.9	-1.1
25	3.4	-2.6	2.4	1.4	-0.6	-1.6	-1.6
26	-2.3	0.7	2.7	2.7	-1.3	-0.3	-2.3
27	-3.1	2.9	6.9	2.9	-3.1	-2.1	-4.1
28	4.8	-4.2	-0.2	-0.2	0.8	0.8	-1.2
29	-5.3	1.7	1.7	2.7	-2.3	0.7	0.7

TABLE III.4 (continued)

	(1)	(2)	(3)	(4)	(5)	(6)	(7)
30	-4.0	1.0	8.0	3.0	-4.0	-2.0	-2.0
31	-2.1	-2.1	-0.1	2.9	0.9	0.9	-0.1
32	-1.9	1.1	5.1	3.1	-3.9	-1.9	-1.9
33	-0.2	-0.2	13.8	4.8	0.0	-2.2	-2.2
34	-0.7	0.3	-6.7	3.3	0.0	3.3	0.3
35	-2.0	0.0	0.0	1.0	-2.0	0.0	3.0
36	1.0	1.0	1.0	0.0	-2.0	0.0	-1.0
37	-1.4	-1.4	5.6	2.6	-0.4	-3.4	-1.4
38	-4.7	2.3	6.3	2.3	-1.7	-1.7	-2.7
39	-2.0	-2.0	5.0	7.0	-7.0	1.0	-2.0
40	-2.1	-0.1	1.9	1.9	-1.1	-0.1	-0.1
41	0.0	0.0	4.0	0.0	0.0	0.0	0.0
42	0.0	0.0	4.5	3.5	0.0	-3.5	-4.5
43	-1.4	1.6	0.6	3.6	-6.4	1.6	0.6
44	0.8	-1.2	1.8	-2.2	3.8	-0.2	-1.2
45	-4.9	1.1	3.1	3.1	-2.9	0.1	0.1
46	-2.6	-1.6	4.4	3.4	-1.6	-0.6	-1.6
47	0.6	0.6	-1.4	1.6	-1.4	0.6	-0.4
48	-5.0	-4.0	5.0	5.0	1.0	0.0	-2.0
49	0.0	1.2	0.2	-0.8	0.2	-0.8	0.2
50	0.0	-1.7	1.3	4.3	-1.7	0.3	-2.7
51	0.0	0.5	-0.5	-2.5	0.5	-0.5	1.5
52	0.0	-1.7	0.3	2.3	1.3	-1.7	-0.7
53	-1.6	-0.6	0.4	2.4	-0.6	0.4	-0.6
54	-1.1	-1.1	1.9	-1.1	2.9	1.9	-3.1
55	1.9	-1.1	-2.1	-0.1	-1.1	1.9	0.9
56	2.0	-2.0	1.0	3.0	-1.0	-2.0	0.0
57	-4.6	2.4	2.4	-1.6	-0.6	0.4	1.4
58	-1.4	-1.4	-1.4	0.6	3.6	0.6	-0.4
59	0.3	0.3	-0.7	2.3	-0.7	-2.7	1.3
60	1.0	1.0	-1.0	-3.0	1.0	1.0	0.0

TABLE III.4 (continued)

	(1)	(2)	(3)	(4)	(5)	(6)	(7)
61	-3.3	-1.3	2.7	0.7	-0.3	1.7	-0.3
62	-1.6	-1.6	1.4	1.4	-0.6	1.4	-0.6
63	2.9	1.9	-3.1	-3.1	1.9	-0.1	-0.1
64	0.0	1.0	5.0	4.0	-1.0	0.0	0.0
65	-1.3	-0.3	-3.3	0.7	0.7	1.7	1.7
66	0.2	-4.8	8.2	4.2	1.2	0.2	-0.8
67	-0.4	0.0	3.6	0.0	-2.4	-0.4	-0.4
68	0.6	0.0	3.6	0.0	-1.4	-2.4	-0.4
69	-4.2	4.8	-4.2	0.0	3.8	-0.2	-0.2
70	2.0	0.0	-1.0	0.0	-2.0	2.0	-1.0
71	0.0	0.0	1.0	0.0	0.0	0.0	-1.0
72	0.0	-0.7	-3.7	0.0	0.0	0.0	4.3
73	0.0	0.0	-2.0	0.0	-1.0	-2.0	5.0
74	0.0	0.0	20.0	0.0	-3.0	-8.0	-9.0
75	-2.0	0.0	1.0	0.0	0.0	2.0	-1.0

III.C. DISTURBANCE DURING THE SCANNING OF SPECTRA AND IRREGULARITY OF THE SCREW

Most of the deleted d_{ij}'s are just statistically bad. But some of them deviate so much from the averaged values that they can be considered as the results of unusual disturbances. It will happen at most once or twice in two days of continuous scanning for our spectrometer. The disturbance is a major nuisance of the scanning of the spectra. But if a spectrum is scanned more than once, the intervals in a spectrum where disturbances occur during a scan can be detected and excluded in processing the data. The intervals where disturbances are believed to have occurred during each of the seven scans are underlined in Tables III.4 and III.5.

For the grating drive, the smoothness of the precision screw may not be identical in every region. If it is possible the region of the precision screw where a bad irregularity is suspected should be avoided. From previous experience, it was found the quality of the first 12 inches of the precision screw, which correspond to a scan of 7 degrees, is better than that of the remaining 6 inches. This is probably due to the fact that this part is used more often. For these seven scans, the first 65 lines are in this range, so the following discussion will concentrate on the calibration in this region.

III.D. CALCULATION OF THE AVERAGE LINE POSITIONS

Since the distance between the neighboring lines is closely related to the difference of their corresponding grating angles, the formula

TABLE III.5

DIFFERENCES BETWEEN LINE POSITIONS AND AVERAGE LINE POSITIONS

	(1)	(2)	(3)	(4)	(5)	(6)	(7)	Average
1	0.0	0.0	0.0	0.0	0.0	0.0	0.0	0.0
2	-15.0	-10.0	4.0	36.0	-20.0	54.0	5.0	9438.0
3	-26.8	-12.8	0.0	37.3	0.0	53.3	7.3	12322.8
4	-22.9	-20.9	7.1	43.1	-27.9	53.1	6.1	15537.9
5	-24.5	-22.5	-2.5	52.5	-31.5	53.5	12.5	18662.5
6	-24.7	-21.7	13.3	56.3	-34.7	52.3	12.3	21704.7
7	-29.1	-22.1	15.9	58.9	-37.1	56.9	9.9	24657.1
8	-30.1	-24.1	21.9	64.9	-44.1	57.9	6.9	27646.1
9	-37.4	-30.4	27.6	72.6	-44.4	58.6	6.6	30317.4
10	-36.7	-35.7	33.3	74.3	-47.7	59.3	6.3	33023.7
11	-36.2	-38.2	39.8	83.8	-50.2	57.8	5.8	35647.2
12	-34.5	-37.5	35.5	87.5	-53.5	60.5	3.5	36438.5
13	-37.9	-38.9	48.1	90.1	-55.9	64.1	4.1	38190.9
14	-40.2	-39.2	52.8	99.8	-59.2	65.8	3.8	40655.2
15	-43.2	-38.2	57.8	103.8	-60.2	64.8	-1.2	43042.2
16	-42.7	-42.7	62.3	109.3	-65.7	0.0	-1.7	45027.7
17	-43.5	-45.5	67.5	132.5	-66.5	69.5	-2.5	47584.5
18	-43.2	-42.2	0.0	133.8	-68.2	66.8	-3.2	49743.2
19	-44.8	-50.8	0.0	137.2	-71.8	71.2	-5.8	51826.8
20	-44.4	-41.4	132.6	137.6	-73.4	71.6	-5.4	53423.4
21	-48.7	-44.7	141.3	149.3	-84.7	77.3	-12.7	61634.7
22	-51.9	-46.9	151.1	156.1	-90.9	77.1	-16.9	69667.9
23	-53.4	-44.4	159.6	159.6	-93.4	76.6	-18.4	72028.4
24	-61.6	-43.6	164.4	166.4	-97.6	77.4	-19.6	76678.6
25	-58.2	-46.2	166.8	167.8	-98.2	75.8	-21.2	77526.2
26	-60.4	-45.4	169.6	170.6	-99.4	75.6	-23.4	81230.4
27	-63.6	-42.6	176.4	173.4	-102.6	73.4	-27.6	85219.6
28	-58.8	-46.8	176.2	173.2	-101.8	74.2	-28.8	85687.8
29	-64.1	-45.1	177.9	175.9	-104.1	74.9	-28.1	90048.1

TABLE III.5 (continued)

	(1)	(2)	(3)	(4)	(5)	(6)	(7)	Average
30	-68.1	-44.1	185.9	178.9	-108.1	72.9	-30.1	92753.1
31	-70.2	-46.2	185.8	181.8	-107.2	73.8	-30.2	94316.2
32	-72.1	-45.1	190.9	184.9	-111.1	71.9	-32.1	98491.1
33	-72.3	-45.3	204.8	189.8	0.0	69.8	-34.3	100127.3
34	-72.9	-44.9	198.1	193.1	-108.9	73.1	-33.9	102576.9
35	-74.9	-44.9	198.1	194.1	-110.9	73.1	-30.9	106575.9
36	-73.9	-43.9	199.1	194.1	-112.9	73.1	-31.9	107347.9
37	-75.4	-45.4	204.6	196.6	-113.4	69.6	-33.4	110487.4
38	-80.1	-43.1	210.9	198.9	-115.1	67.9	-36.1	114424.1
39	-82.1	-45.1	215.9	205.9	-122.1	68.9	-38.1	118059.1
40	-84.3	-45.3	217.8	207.8	-123.3	68.8	-38.3	121358.3
41	0.0	0.0	221.8	207.8	0.0	68.8	-38.3	121721.3
42	-86.8	-45.8	226.3	211.3	-129.8	65.3	-42.8	125303.8
43	-88.1	-44.1	226.9	214.9	-136.1	66.9	-42.1	128153.1
44	-87.4	-45.4	228.6	212.6	-132.4	66.6	-43.4	128806.4
45	-92.2	-44.2	231.8	215.8	-135.2	66.8	-43.2	132230.2
46	-94.8	-45.8	236.2	219.2	-136.8	66.2	-44.8	134816.8
47	-94.2	-45.2	234.8	220.8	-138.2	66.8	-45.2	135578.2
48	-99.2	-49.2	239.8	225.8	-137.2	66.8	-47.2	141342.2
49	0.0	-48.1	239.9	224.9	-137.1	65.9	-47.1	142047.1
50	-104.7	-49.7	241.3	229.3	-138.7	66.3	-49.7	147753.7
51	0.0	-49.2	240.8	226.8	-138.2	65.8	-48.2	148222.2
52	-108.9	-50.9	241.1	229.1	-136.9	64.1	-48.9	151201.9
53	-110.4	-51.4	241.6	231.6	-137.4	64.6	-49.4	154037.4
54	-111.6	-52.6	243.4	230.4	-134.6	66.4	-52.6	156946.6
55	-109.8	-53.8	241.3	230.3	-135.8	68.3	-51.8	159716.8
56	-107.8	-55.8	242.3	233.3	-136.8	66.3	-51.8	160200.8
57	-112.3	-53.3	244.7	231.7	-137.3	66.7	-50.3	162418.3
58	-113.8	-54.8	243.3	232.3	-133.8	67.3	-50.8	165050.8
59	-113.4	-54.4	242.6	234.6	-134.4	64.6	-49.4	167618.4
60	-112.4	-53.4	241.6	231.6	-133.4	65.6	-49.4	170115.4

TABLE III.5 (continued)

	(1)	(2)	(3)	(4)	(5)	(6)	(7)	Average
61	-115.8	-54.8	244.3	232.3	-133.8	67.3	-49.8	172178.8
62	-117.3	-56.3	245.7	233.7	-134.3	68.7	-50.3	174920.3
63	-114.4	-54.4	242.6	230.6	-132.4	68.6	-50.4	177223.4
64	-114.4	-53.4	247.6	234.6	-133.4	68.6	-50.4	177996.4
65	-115.3	-53.8	244.3	235.3	-132.8	70.3	-48.8	179460.8
66	-115.6	-58.6	252.4	239.4	-131.6	70.4	-49.6	181636.6
67	-115.9	0.0	256.1	0.0	-133.9	70.1	-49.9	183697.9
68	-115.4	-57.4	259.6	0.0	-135.4	67.6	-50.4	185802.4
69	-119.5	-52.5	255.5	0.0	-131.5	67.5	-50.5	187791.5
70	-117.5	0.0	254.5	0.0	-133.5	69.5	-51.5	189301.5
71	0.0	-59.5	255.5	0.0	0.0	0.0	-52.5	189730.5
72	-128.2	-60.2	251.8	0.0	-131.2	72.8	-48.2	191593.2
73	0.0	0.0	249.8	0.0	-132.2	70.8	-43.2	193401.2
74	-125.2	0.0	269.8	0.0	-135.2	62.8	-52.2	200186.2
75	-127.2	0.0	270.8	0.0	-135.2	64.8	-53.2	205479.2

used to calculate the average line positions, which will be denoted by $\overline{X}_i$, must preserve the distance between two neighboring lines, namely, $\overline{X}_i - \overline{X}_{i-1} \approx \overline{d}_i$.

If $\overline{X}_i$ is calculated by using the averaged distance between two neighboring lines, that is,

$$\overline{X}_i = \sum_{k=1}^{i} \overline{d}_k \tag{3.1}$$

then

$$\overline{X}_i - \overline{X}_{i-1} = \overline{d}_i \ .$$

The distance between two neighboring lines will not be different from $\overline{d}_i$ by more than 0.3%.

If $\overline{X}_i$ is calculated by averaging the available X_{ij} values, the formula can be written as

$$\overline{X}_i = \frac{\sum_{j=1}^{n} W_{ij} X_{ij}}{\sum_{j=1}^{n} W_{ij}} \tag{3.2}$$

where

$W_{ij} = 1$ if $X_{ij} \neq 0$,

$W_{ij} = 0$ if $X_{ij} = 0$.

This formula seems to be very reasonable. But it should be checked if anything unreasonable should occur. Assume $X_{ij} \neq 0$ for $j = 1$ to n and $X_{i-1,j} \neq 0$ for $j \neq k$. Then the expression for $\overline{X}_i - \overline{X}_{i-1}$ is

$$\bar{X}_i - \bar{X}_{i-1} = \frac{\sum_{j=1}^{n} X_{ij}}{n} - \frac{\sum_{\substack{j=1 \\ j\neq k}}^{n} X_{i-1,j}}{n-1}$$

$$= \left(\frac{\sum_{j=1}^{n} X_{ij}}{n} - \frac{\sum_{\substack{j=1 \\ j\neq k}}^{n} X_{ij}}{n-1} \right) + \left(\frac{\sum_{\substack{j=1 \\ j\neq k}}^{n} X_{ij}}{n-1} - \frac{\sum_{\substack{j=1 \\ j\neq k}}^{n} X_{i-1,j}}{n-1} \right)$$

$$= \frac{\sum_{j=1}^{n} (n-1)X_{ij} - \sum_{\substack{j=1 \\ j\neq k}}^{n} nX_{ij}}{n(n-1)} + \frac{\sum_{\substack{j=1 \\ j\neq k}}^{n} (X_{ij} - X_{i-1,j})}{N_L}$$

$$= \frac{\sum_{\substack{j=1 \\ j\neq k}}^{n} (n-1)X_{ij} + (n-1)X_{ik} + \sum_{\substack{j=1 \\ j\neq k}}^{n} nX_{ij}}{n(n-1)} + \frac{\sum_{\substack{j=1 \\ j\neq k}}^{n} (X_{ij} - X_{i-1,j})}{n-1}$$

$$= \frac{\sum_{\substack{j=1 \\ j\neq k}}^{n} X_{ij} + (n-1)\, X_{ik}}{n(n-1)} + \frac{\sum_{\substack{j=1 \\ j\neq k}}^{n} (X_{ij} - X_{i-1,j})}{n(n-1)}$$

$$= \frac{X_{ik} - \bar{X}_i}{n} + \frac{\sum_{\substack{j=1 \\ j\neq k}}^{n} (X_{ij} - X_{i-1,j})}{n-1}$$

$$\approx \frac{X_{ik} - \bar{X}_i}{n} + \bar{d}_i \,. \qquad (3.3)$$

From the discussion presented in Appendix A, the first term can be very large when X_{ik} is large. The value for $\bar{X}_i - \bar{X}_{i-1}$ obtained by

Eq. (3.2) can deviate from $\bar{d}_i$ by a large number; this is not acceptable. Therefore Eq. (3.1) will be used to obtain the average line positions; these are listed in column 8 of Table III.5, p. 30. Columns 1 to 7 of Table III.5 are the values for $X_{ij} - \bar{X}_i$. Examining the values in each column, the values for $X_{ij} - \bar{X}_i$ really tend to increase as the value of X_{ij} is increased as predicted by the results of Appendix A.

III.E. RESCALED AVERAGE LINE POSITIONS

The average line positions obtained in the previous sections are still slightly biased. When the ith line in the jth scan is missing, the value for d_{ij} is not available and the value for $\bar{d}_i$ is obtained from the other d_{ij}'s. Since $\frac{\Delta\theta}{\Delta x}$ is usually changing slowly for a particular scan, it is consistently faster or slower than the average scan in a short range. Without a particular d_{ij}, the obtained average line position $\bar{d}_i$ will be biased compared to $\bar{d}_{i+1}$ and $\bar{d}_{i-1}$, where all the values of d_{ij}'s are available.

It is possible to suppress this biasing effect by reducing the differences among these scans. By rescaling the line positions for all these scans to make the last line position, X_{fj}, equal to a fixed value, we practically change no information contained in a particular scan. But the effective speeds of grating rotation will be close to each other for these scaled scans. The biasing effect due to the unavailable values of d_{ij}'s is thus reduced. After the rescaled line positions are obtained, the rescaled average line position can be similarly defined.

The effect of the rescaling on the calibration will be seen later. The rescaled average line positions and the rescaled $(X_{ij} - \overline{X}_i)$'s are listed in Table III.6.

III.F. CO 1←0 BAND

When more than one scan of the same calibrated spectrum have been recorded, it is possible to obtain the statistically improved results by applying interpolation procedures to each of the scans and then average the wavenumbers obtained for a spectral line. (This will be referred to as method A.) On the other hand, the average line positions can be used to obtain an average interpolation function. (This will be referred to as method B.) In Appendix B, it is proved that method B can yield as good or better results than method A. Of course, the correct method to obtain the average line positions in Section III.3 should be used and the biasing effect should be avoided. Considering (2←0) lines as calibration lines and using the least squares fitting programs developed by Kurlat (9), and Hafford (10), the following methods have been used to determine the wavenumbers for the CO 1←0 band:

1. Equation (1.5) is used as the interpolation equation to fit each scan separately. The wavenumbers of a particular line are then averaged to obtain statistically improved results.

2. Equation (1.5) is used as the interpolation equation to relate the average line positions or the rescaled average line positions to the wavenumber scale.

TABLE III.6

DIFFERENCES BETWEEN RESCALED LINE POSITIONS AND RESCALED AVERAGE LINE POSITIONS

	(1)	(2)	(3)	(4)	(5)	(6)	(7)	Average
1	0.0	0.0	0.0	0.0	0.0	0.0	0.0	0.0
2	-7.8	-6.0	-7.7	24.7	-11.9	51.4	8.7	9436.8
3	-15.1	-5.3	0.0	24.8	0.0	52.2	14.4	12318.9
4	-8.9	-12.2	-10.0	26.7	-12.4	51.0	14.4	15533.8
5	-10.2	-14.6	-25.5	30.3	-15.4	48.5	19.9	18660.1
6	-8.5	-13.0	-14.0	30.1	-16.4	46.0	20.4	21702.3
7	-10.5	-12.0	-15.0	29.2	-16.2	49.9	19.3	24654.3
8	-9.1	-12.7	-12.6	31.8	-20.5	50.2	17.6	27642.8
9	-14.3	-17.7	-10.0	36.4	-18.4	50.3	18.4	30313.6
10	-11.4	-21.8	-7.6	35.0	-19.3	50.4	19.3	33019.5
11	-10.1	-24.4	-5.6	40.1	-20.8	46.9	18.6	35643.9
12	-7.4	-22.9	-10.4	43.4	-22.9	49.9	17.1	36434.6
13	-9.6	-23.8	-0.2	43.7	-24.0	52.8	18.1	38187.0
14	-11.4	-24.4	0.1	49.1	-26.5	52.5	17.5	40652.3
15	-12.5	-22.3	2.2	50.3	-25.4	51.0	13.5	43038.9
16	-10.4	-26.0	4.3	53.5	-29.2	0.0	13.8	45024.2
17	-9.9	-28.3	5.7	73.0	-28.4	53.8	13.4	47581.3
18	-8.3	-24.4	0.0	71.4	-28.5	50.2	13.2	49740.0
19	-8.5	-32.4	0.0	72.1	-30.6	53.8	11.2	51823.6
20	-7.1	-22.5	62.7	70.4	-31.0	53.6	12.0	53420.2
21	-4.8	-22.0	61.6	72.7	-34.9	57.4	8.3	61630.1
22	-1.6	-20.6	61.7	70.2	-33.9	55.3	7.5	69662.0
23	-2.4	-18.2	66.1	69.8	-35.5	53.1	5.8	72023.3
24	-6.8	-15.3	65.4	71.2	-35.6	52.8	6.6	76672.8
25	-2.2	-16.9	67.3	72.2	-34.8	51.6	5.9	77519.6
26	-1.5	-14.5	65.6	70.6	-32.8	50.4	5.3	81223.3
27	-1.4	-9.8	67.6	68.9	-32.3	47.3	2.8	85211.8
28	3.9	-13.7	67.0	68.3	-31.0	48.1	1.9	85679.8
29	2.1	-10.0	63.4	66.0	-29.4	47.8	4.6	90039.4

TABLE III.6 (continued)

	(1)	(2)	(3)	(4)	(5)	(6)	(7)	Average
30	0.3	-7.8	68.2	65.9	-30.9	45.2	3.7	92743.9
31	-0.6	-9.1	66.2	66.9	-28.7	45.7	4.3	94306.8
32	0.9	-6.1	66.3	65.3	-28.8	42.9	4.2	98481.0
33	1.9	-5.6	78.1	68.1	0.0	40.2	2.6	100117.0
34	1.7	-5.7	66.9	67.1	-24.6	41.5	2.5	102567.8
35	2.9	-3.9	62.1	63.4	-23.0	40.5	7.2	106566.1
36	4.5	-2.5	62.2	62.6	-24.3	40.3	6.5	107338.0
37	5.6	-2.4	64.0	61.6	-21.9	36.2	6.5	110476.9
38	4.1	1.6	65.6	59.3	-20.0	33.6	5.4	114412.9
39	5.0	1.3	66.2	62.1	-23.8	33.7	5.0	118047.4
40	5.4	2.6	64.1	60.1	-22.0	32.8	6.3	121346.0
41	0.0	0.0	67.6	59.7	0.0	32.6	6.4	121709.0
42	8.1	5.8	69.7	61.0	-23.1	30.3	5.4	125288.9
43	8.9	8.8	66.9	61.3	-26.9	31.2	7.2	128137.9
44	10.2	7.8	67.9	58.3	-22.6	30.8	6.3	128791.0
45	8.1	10.5	66.9	57.5	-22.3	30.1	7.8	132214.3
46	7.6	10.1	68.1	57.9	-21.6	28.9	7.3	134800.5
47	8.4	10.6	65.4	58.3	-22.8	28.9	6.8	135562.2
48	8.0	9.3	63.6	56.6	-16.5	27.6	7.4	141325.2
49	0.0	10.9	62.9	55.1	-15.6	26.8	7.9	142029.8
50	8.5	12.6	58.2	53.6	-11.4	26.5	8.4	147734.8
51	0.0	13.3	57.2	50.6	-10.5	25.9	10.2	148203.2
52	7.5	13.4	54.3	49.9	-6.1	23.9	11.2	151182.0
53	8.2	14.1	51.3	49.0	-4.1	23.7	11.8	154017.1
54	9.4	14.3	49.7	44.6	1.4	24.9	9.9	156925.8
55	13.5	14.4	44.3	41.3	2.7	26.1	12.0	159695.4
56	15.9	12.6	44.6	43.7	2.1	24.0	12.2	160179.4
57	13.1	16.1	44.4	39.5	3.5	23.9	14.6	162396.6
58	13.8	15.8	39.8	37.1	9.4	23.8	15.3	165028.6
59	16.1	17.3	35.9	36.4	11.0	20.5	17.6	167595.9
60	19.1	19.4	32.0	30.5	14.3	20.9	18.8	170092.5

TABLE III.6 (continued)

	(1)	(2)	(3)	(4)	(5)	(6)	(7)	Average
61	17.5	19.1	32.2	28.9	15.9	22.2	19.3	172155.4
62	18.1	18.8	30.4	27.1	17.8	22.9	19.9	174896.6
63	22.8	21.7	24.4	21.4	21.7	22.3	20.8	177199.3
64	22.5	22.3	27.7	23.6	20.6	21.3	20.3	177973.0
65	21.7	21.8	21.8	21.8	21.8	21.8	21.8	179437.9
66	22.4	16.8	26.2	22.3	23.7	20.3	20.8	181614.6
67	23.4	0.0	27.1	0.0	22.9	19.1	20.9	183675.9
68	25.4	19.3	27.8	0.0	23.1	15.9	21.1	185780.3
69	21.0	23.3	19.4	0.0	26.9	13.5	20.1	187770.9
70	24.0	0.0	16.4	0.0	26.0	14.9	19.4	189280.9
71	0.0	17.1	17.1	0.0	0.0	0.0	18.8	189709.6
72	12.5	14.6	8.4	0.0	27.9	15.2	21.3	191574.7
73	0.0	0.0	6.3	0.0	30.5	14.8	29.1	193380.4
74	24.8	0.0	18.3	0.0	33.8	5.4	23.2	200164.1
75	26.3	0.0	12.3	0.0	37.8	5.4	23.7	205456.9

3. Consider CO 2←0 lines as grating angle markers and use Eq. (1.2) to obtain the angles to correspond to each CO 2←0 line. Each $\overline{X}_i$ as the line position scale, and use a simple linear interpolation procedure to calculate the grating angles for each CO 1←0 line. Then the grating equation is used to obtain the wavenumbers.

In method 2 both the average line positions and the rescaled average line positions are used in the fits and the standard deviations are 0.0021 cm^{-1} and 0.0012 cm^{-1}, respectively. The rescaled average line positions yield considerably better results, which is consistent with the discussion in Section III.E. The results obtained by using the rescaled average line position will be considered as the results by method 2 in the following discussion.

The wavenumbers of the CO 1←0 band obtained by these methods are compared with the wavenumbers measured by Guelachevili (3). Allowing some systematic error to be subtracted out, the comparison is done by evaluating the variance, denoted by V, of our measured wavenumbers, which is defined to be

$$V = \frac{\sum_{i=1}^{22} [\nu_i - \nu_{Gi} - A - B(\nu_i - 2143)]}{22} \qquad (3.7)$$

where ν_{Gi}'s are the wavenumbers measured by Guelachevili and A - B (ν_i-2143) represents the systematic error and A, B are determined by least-squares regression analysis. The values of V for these methods are 7.1 x 10^{-7} $(cm^{-1})^2$, 3.51 x 10^{-7} $(cm^{-1})^2$, 4.2 x 10^{-7} $(cm^{-1})^2$, respectively. Method 2 yields the least value of V, so it yields the

best calculated CO 1←0 wavenumbers. The systematic error determined by method 2 is about 0.0027 cm^{-1}. The reason for this systematic error is possibly due to the difference that exists in the response function of the instrument in different orders.

The accuracy of a calculated wavenumber by method 2 is 1 part in 3.3×10^6.

III.G. DETERMINATION OF THE PROPER DENSITY OF THE CALIBRATION LINES

It takes at least 3 scans to obtain filtered average line positions. And it seems to be appropriate to have 3 calibrated scans to obtain the statistically improved calculated wavenumbers. So the proper density of the calibration lines by 3 scans will be discussed.

Since there are very few lines unobserved in scans 5, 6, and 7, they are chosen to represent 3 well-calibrated spectra. (The results by the average line positions are found to be close to the results by the rescaled average line positions in this case.)

The number of the calibration lines is assumed to be 43, 22, 16, and 11 to obtain calibration equations f_1, f_2, f_3, f_4, respectively. The standard deviations of the fits, denoted by σ_1, σ_2, σ_3, σ_4, are equal to 0.0013 cm^{-1}, 0.0013 cm^{-1}, 0.0033 cm^{-1}, 0.0027 cm^{-1}, respectively. Only σ_1 and σ_2 are close to each other, so only those two corresponding densities of the calibration lines are possibly greater than the proper density of the calibration lines. The variance of (f_1-f_2) is 4.9×10^{-8} $(cm^{-1})^2$, which is about 3% of the variance of the

fits, which is much less than the 20% criterion. With this evidence, it can be said that 22 calibration lines in this range of the spectra is sufficient to minimize the error due to the variation of the speed of the rotation of the grating and the irregularity of the precision screw within 0.00022 cm^{-1}. The variances for (f_1-f_3) and (f_1-f_4) are found to be 0.0027 cm^{-1} and 0.0028 cm^{-1}, respectively. Both of these values are greater than σ_1.

The calculated wavenumbers for the CO 1←0 band by f_1 are compared with Guelachvili's results. With the systematic error subtracted out, the standard deviation is 0.00095 cm^{-1} which corresponds to the accuracy of 1 part in 2.2×10^6.

III.H. CONCLUSIONS

The investigations presented in this study for the measurement error and the interpolation error are quite helpful in the determination of the reliability of a calibration procedure.

The procedures used here, which are trivial in many aspects, to analyze a spectrometric system can be used to examine the reproducibility of a new system to operate or when questions arise concerning the operation of the instrument. The concept of the proper density of calibration lines is particularly useful when different calibration techniques are contemplated.

PART II

AN ANALYSIS OF $\nu_9 + \nu_{12}$, C_2H_6

CHAPTER IV

VIBRATION-ROTATION THEORY FOR MOLECULES WITH THREEFOLD AXIAL SYMMETRY

IV.A. THE CLASSICAL KINETIC ENERGY (11,12,13)

A polyatomic molecule is a system containing N nuclei and n electrons. If the intrinsic spins are neglected, the system can be regarded as a system of N + n particles with 3 (N + n) degrees of freedom. The Born-Oppenheimer approximation (14) allows one to treat, in general, the electronic motions and the motions of the nuclei separately. Furthermore three degrees of freedom correspond to the translation of the center of mass. The remaining 3N - 3 degrees of freedom are considered in the description of the rotation and vibration of the molecule.

The rotation for a nonlinear molecule can be described with three angular coordinates which describe the orientation of the "body-fixed" coordinate system with respect to a space-fixed coordinate system. The "body-fixed" coordinate system is usually chosen such that the inertia tensor for the rigid molecule is diagonal. The rotational angular momentum is given by

$$\underline{P} = \underline{\underline{I}} \cdot \underline{W}$$

where $\underline{\underline{I}}$ is the inertia tensor and $\underline{W}$ is the angular velocity of the body-fixed frame.

The vibration of the molecule is described with the remaining 3N - 6 degrees of freedom. Assuming small displacements, the normal coordinates of the system, $Q_{s\sigma}$, can be found and are related to the 3N mass adjusted cartesian displacements of the nuclei, $\sqrt{M_i}\ \Delta\alpha_i (\alpha = x,y,z)$, by

$$Q_{s\sigma} = \sum_{i=1}^{N} \sum_{\alpha} (\ell^{\alpha}_{is\sigma})^{-1}\ \sqrt{M_i}\ \Delta\alpha_i$$

where s denotes the normal mode of vibration, σ distinguishes the degenerate components of mode s, and i labels the nuclei. The conjugate momentum of $Q_{s\sigma}$ is given in terms of the kinetic energy by

$$P^{*}_{s\sigma} = \frac{\partial T}{\partial \dot{Q}_{s\sigma}} .$$

The components of angular momentum arising from vibration are given by

$$P_{\alpha} = \sum_{s\sigma} \sum_{s'\sigma'}{}' \zeta^{\alpha}_{s\sigma s'\sigma'}\ Q_{s\sigma}\ P^{*}_{s'\sigma'}$$

where $\zeta^{\alpha}_{s\sigma s'\sigma'}$ is the Coriolis coupling constant connecting the vibration $s\sigma$ and $s'\sigma'$ with rotations about the α axis of the "body-fixed coordinate system and is defined by

$$\zeta^{\alpha}_{s\sigma s'\sigma} = \sum_{i=1}^{N} (\ell^{\beta}_{is\sigma}\ \ell^{\gamma}_{is'\sigma'} - \ell^{\gamma}_{is\sigma}\ \ell^{\beta}_{is'\sigma'})$$

where α, β, γ occur cyclically and $\ell^{\gamma}_{is\sigma}$ are coefficients of the matrix which transform weighted Cartesian to normal coordinates. The classical kinetic energy expressed in complete Hamiltonian form can be written

$$T = \frac{1}{2} \sum_{\alpha\beta} \mu_{\alpha\beta} (P_\alpha - p_\alpha)(P_\alpha - p_\alpha) + \frac{1}{2} \sum_{s\sigma} P^{*2}_{s\sigma}$$

where $\mu_{\alpha\beta}$'s are functions of the inertia tensor elements and the $\ell^{\alpha}_{s\sigma s'\sigma'}$'s.

IV.B. QUANTUM-MECHANICAL HAMILTONIAN

The quantum mechanical formulation of the Hamiltonian has been derived by Wilson and Howard (12), Darling and Dennison (15), and recently by Watson (16). All these treatments give equivalent expressions for the Hamiltonian. The final form given by Watson is

$$H = \frac{1}{2} \sum_{\alpha\beta} (P_\alpha - p_\alpha)\, \mu_{\alpha\beta} (P_\beta - p_\beta) + \frac{1}{2} \sum_{s\sigma} P^{*2}_{s} + U + V$$

in which V is the potential energy and U is a complicated function of the coordinates and, in general, is small compared to V. V is usually expanded by a Taylor series in the normal coordinates, $Q_{s\sigma}$:

$$V = \frac{1}{2} \sum_{s\sigma} \lambda_s Q^2_{s\sigma} + \sum_{s\sigma} \sum_{s'\sigma'} \sum_{s''\sigma''} K_{s\sigma s'\sigma' s''\sigma''} Q_{s\sigma} Q_{s'\sigma'} Q_{s''\sigma''} + \cdots$$

It is very difficult to solve the wave equation,

$$(H - E)\, \psi = 0$$

exactly. A systematic approximation method has been carried out by Goldsmith, Amat and Nielsen (17-22) and by Tarrago (23) for the particular case of threefold axial symmetry. The Hamiltonian is expanded in orders of magnitude

$$H = H_0 + H_1 + H_2 + H_3 \ldots$$

The first term, H_0, has the form

$$H_0 = \frac{1}{2} \sum_{\alpha} \frac{P_\alpha^2}{I_\alpha} + \frac{1}{2} \sum_{s\sigma} [P^*_{s\sigma}{}^2 + \lambda_s Q^2_{s\sigma}].$$

For molecules with axial symmetry ($I_x = I_y + I_z$), the zero order Schrödinger equation

$$H_0\psi = E_0\psi$$

has well-known analytic solutions (11). The eigenfunctions are denoted by

$$|\psi> = |\psi_R>|\psi_V>$$

where $|\psi_R> = |j,k>$

and $|\psi_V> = |V_1> \ldots |V_n> \ldots |V_t,\ell_t>$.

Here, j and k are angular momentum quantum numbers, V_s is a vibration quantum number, and ℓ_t is a quantum number associated with the vibrational angular momentum in the degenerate vibrational state denoted by t. E_0 is given by

$$E_0 = E_R + E_V$$

$$= B_e J(J+1) + (A_e - B_e)K^2 + \Sigma\omega_s(V_s + \frac{g_s}{2}) \ .$$

IV.C. VIBRATION-ROTATION THROUGH FOURTH ORDER

To obtain more accurate solutions for the rotation-vibration Hamiltonian H, higher order terms have to be considered. A contact transformation can be made on the Hamiltonian such that the resulting Hamiltonian (11)

$$h' = H_0 + h_1' + h_2' + h_3' + \ldots$$

is diagonal, through h_1', with respect to all quantum numbers for axially symmetric molecules. Amat and Nielsen (20-22) performed a second contact transformation which diagonalized h' through second order with respect to the vibrational quantum number V_5. For axially symmetric molecules, the twice transformed Hamiltonian

$$h^+ = H_0 + h_1' + h_2' + h_3' + h_4' + \ldots$$

is diagonal with respect to the vibrational quantum numbers through h_2^+. The energies obtained from the twice transformed Hamiltonian using H_0, h', and diagonal elements of h_2^+ are normally good through third order except in case of resonance (24).

Table IV.1 gives the complete vibration-rotation energy for the case of axial symmetry through third order, with some correction terms occurring in fourth order for $K \approx J \approx 30$ (23,25). More general results can be found in the book by Amat, Nielsen and Tarrago (26).

TABLE IV.1

ENERGY FOR AXIALLY SYMMETRIC MOLECULES

Term	Energy
H_o	$B_e J(J+1)+(A_e-B_e)K^2 + \sum \omega_s (v_s+ \frac{g_s}{2})$
h_1'	$-2A_e \sum \zeta_t^z \ell_t K$
h_2''	$-D_e^J J^2(J+1)^2-D_e^{JK}K^2J(J+1)-D_e^K K^4$ $-\sum \alpha_s^B (v_s+ \frac{g_s}{2})J(J+1) - \sum (\alpha_s^A-\alpha_s^B)(v_s+ \frac{g_s}{2})K^2$ $+\sum x_{ss'}(v_s+ \frac{g_s}{2})(v_s'+ \frac{g_{s'}}{2}) + \sum x_{\ell_t\ell_{t'},\ell_t\ell_{t'}}$
h_3''	$+\sum \ell_t \eta_{tJ} J(J+1)K + \sum \ell_t \eta_{tK} K^3 + \sum \ell_t [\eta_t+ \sum \eta_{ts}(v_s+ \frac{g_s}{2})]K$
h_4''	$+ \sum \beta_s^J [v_s+ \frac{g_s}{2}] J^2[J+1]^2 + \sum \beta_s^{JK}[v_s+ \frac{g_s}{2}]J[J+1]K^2 + \sum \beta_s^K K^4[v_s$ $+ \frac{g_s}{2}] + \left\{ \sum \gamma_{ss'}^b [v_s+ \frac{g_s}{2}][v_{s'}+ \frac{g_{s'}}{2}]+\sum \gamma^B_{\ell_t\ell_{t'},t\ell_{t'}}+\Delta B_e^{(a)} \right\}$ $\{J[J+1]-K^2\}+ \left\{ \sum \gamma_{ss'}^A [v_s+ \frac{g_s}{2}][v_{s'}+ \frac{g_{s'}}{2}]+ \sum \gamma^A_{\ell_t\ell_{t'},t\ell_{t'}}+\Delta A_e^{(a)} \right\}K^2$ $+\sum Y_{ss's''}[v_s+ \frac{g_s}{2}][v_{s'}+ \frac{g_{s'}}{2}][v_{s''}+ \frac{g_{s''}}{2}]+ \sum Y_{s\ell_t\ell_{t'},\ell_t\ell_{t'}}[v_s+ \frac{g_s}{2}]$ $+\sum \Delta\omega_s[v_s+ \frac{g_s}{2}]+H_o^J J^3(J+1)^3+H_o^{JK}J^2(J+1)^2K^2+H_o^{KJ}J(J+1)K^4+H_o^K K^6$

IV.D. RESONANCES

Many resonances important in rotation-vibration spectra may be usefully classified as vibrational, rotational, or as vibration-rotation resonances. The first are those that are diagonal in all rotational quantum numbers and off-diagonal only in the vibrational quantum numbers. Fermi resonance is an example of this type of resonance (28). The second are diagonal in all the vibrational quantum numbers and off-diagonal only in the rotational quantum numbers. The most common and most important is the so-called ℓ-type doubling (27,28). The third are off-diagonal in both the vibrational and rotational quantum numbers. Such resonances are usually called "Coriolis resonances" (26,28,29).

All resonances are important in determining the detailed structure of the rotation-vibration energies of polyatomic molecules.

IV.E. MOLECULAR SYMMETRY GROUP AND CLASSIFICATION OF ENERGY LEVELS FOR SYMMETRIC-TOP MOLECULES

Group representation theory has long been found to be very useful in the study of molecular spectroscopy. Hougen (30) showed how to classify the rotation-vibration energy levels of a rigid nonlinear molecule according to the species labels of the molecular point group. Longuet-Higgins (31) suggested that the symmetry group of a molecule as the set of (1) all feasible permutations of the positions and spins of identical nuclei and (2) all feasible permutation-inversions, which simultaneously invert the coordinates of all particles through the

center of mass. Using representations of such groups, it is possible to classify the rovibronic (rotation-vibration-electronic) energy levels for both rigid and nonrigid molecules.

The existing rotation-vibration energy levels for symmetric-top molecules are usually given four labels: J, specifying the total angular momentum; K, specifying the component of the angular moment about the top axis; $+\ell$ or $-\ell$, labels arising from a consideration of Coriolis splittings in degenerate vibronic states; and Γ, a symmetry species of the molecule group.

The classification of rotation-vibration energy levels is very useful in determining the nonvanishing elements of a physical operator. For example, using the symmetry considerations, it is found that the electric dipole transition between two rovibronic states, of species Γ' and Γ'', is allowed if and only if $\Gamma' \times \Gamma''$ contains $\Gamma_{T_z} \times \Gamma_{R_z}$. ($\Gamma_{T_z}$ and Γ_{R_z} are the species of the translation in the z direction and the rotation about z axis.)

IV.F. SELECTION RULES

For an electric dipole absorption transition between two states a and b to be observable it is required that at least one of three matrix elements

$$\langle a | M_\alpha | b \rangle$$

must be nonzero, where M_α is one of the x, y, z components of the dipole moment. Using the zero-order wave functions for the axially symmetric molecules, the selection rules are:

1. For transition moments parallel to the symmetry axis

$\Delta K = 0$

$\Delta J = 0, \pm 1$ if $K \neq 0$

$\Delta J = \pm 1$ if $K = 0$

2. For transition moments perpendicular to the symmetry axis

$K = \pm 1$

$J = 0, \pm 1$

When higher order Hamiltonian terms are used to obtain more correct wave functions, further selection rules have to be obtained. The case of threefold axial symmetry has been examined by Tarrago (23) and the selection rules are given in Table IV.2

IV.G. INTENSITIES OF TRANSITIONS

The intensities of those allowed transitions are

$$I = \nu C\ G\ F(K,J,\Delta K,\Delta J)\ \exp[-E_0(K,J)/KJ]$$

where ν is the transition frequency, C is a proportionality factor which depends on the vibrational transition, G is a statistical weight which depends on the nuclear spin state and the degeneracy of the ground state, and $E_0(K,J)$ is the ground state energy. K and J refer to the rotational quantum number of the ground state. T is the absolute temperature and K is the Boltzmann constant. F(K, J, ΔK, ΔJ) is the transition moment.

For symmetric top molecules F is given as follows (28):

TABLE IV.2

SYMMETRY SELECTION RULES FOR C_{3v} MOLECULES (23)

		$\sum_t \Delta\ell_t + \sum_{n(A_2)} \Delta v_n$ even	$\sum_t \Delta\ell_t + \sum_{n(A_2)} \Delta v_n$ odd
Parallel Bands $\sum_t \Delta\ell_t = 3p$ $\Delta K = 0$	Q Branches $\Delta J = 0$	$\|+\rangle \leftrightarrow \|-\rangle$	$\|+\rangle \leftrightarrow \|+\rangle$ [a] $\|-\rangle \leftrightarrow \|-\rangle$
	R and P Branches $\Delta J = \pm 1$	$\|+\rangle \leftrightarrow \|+\rangle$ $\|-\rangle \leftrightarrow \|-\rangle$	$\|+\rangle \leftrightarrow \|-\rangle$
Perpendicular Bands $\sum \Delta\ell_t - \Delta K = 3p$ $\Delta K = \pm 1$	Q Branches $\Delta J = 0$	$\|+\rangle \leftrightarrow \|+\rangle$ $\|-\rangle \leftrightarrow \|-\rangle$	$\|+\rangle \leftrightarrow \|-\rangle$
	R and P Branches $\Delta J = \pm 1$	$\|+\rangle \leftrightarrow \|-\rangle$	$\|+\rangle \leftrightarrow \|+\rangle$ $\|-\rangle \leftrightarrow \|-\rangle$
$A_1 \leftrightarrow A_2$; $E \leftrightarrow E$			

[a] 1+ and 1- refer to symmetry adapted wavefunctions (26,32).

1. For K = 0 (parallel bands)

$$F(K,J,0,\Delta J) = \begin{cases} \dfrac{(J+1)^2-K^2}{(J+1)(2J+1)} & \text{if } \Delta J = +1 \\ \dfrac{K^2}{J(J+1)} & \text{if } \Delta J = 0 \\ \dfrac{(J^2-K^2)}{2(2J+1)} & \text{if } \Delta J = -1 \end{cases}$$

2. For K = 1 (perpendicular bands)

$$F(K,J,\pm 1,\Delta J) = \begin{cases} \dfrac{(J+2+K\Delta K)(J+1+K\Delta K)}{(J+1)(2J+1)} & \text{if } J = +1 \\ \dfrac{(J+1+K\Delta K)(J-K\Delta K)}{J(J+1)} & \text{if } J = 0 \\ \dfrac{(J-1-K\Delta K)(J-K\Delta K)}{2(2J+1)} & \text{if } J = -1 \end{cases}$$

The statistical weight G for threefold axial symmetric molecule is (25,28)

$$G = (2-\delta_{k,0})(2J+1)\left(1 + \frac{3}{4s(s+1)}\,\delta_{K,3N}\right)$$

where s is the spin of each of the three identical nuclei, δ_i, j is the Kronecker delta, and n is an integer.

IV.H. TRANSITION FREQUENCIES

The energy of a rotation-vibration state, through second order, is

$$E(\{V_s\},\{\ell_t\},J,K) = E_V + B_0J(J+1) + (A_0-B_0)K^2$$

$$-2A_e \sum_t \zeta_t^2 \ell_t K - D_0^J J^2(J+1)^2 - D_0^{JK} K^2 J(J+1)$$

$$- D_0^K K^4 - \sum_s \alpha_s^B V_s J(J+1) - \sum_s [\alpha_s^A - \alpha_s^B] V_s K^2$$

where E_V is the vibrational energy. The ground state energy is

$$E(\{0\},\{0\},J,K) = E_{V0} + B_0J(J+1) + (A_0-B_0)K^2 - D_0^J J^2(J+1)^2$$

$$- D_0^J J^2(J+1)^2 - D_0^{JK} K^2 J(J+1) - D_0^K K^4 .$$

The frequency of a transition from the ground state to an excited state is then given by (25,27)

$$E(\{V_s\},\{\ell_t\},J+\Delta J,K+\Delta K) - E(\{0\},\{0\},J,K) = {}^{\Delta K}\Delta J_K(J)$$

$$= V_0 + B_0(2J+\Delta J+1)\Delta J + (A_0-B_0)(2K+\Delta K)\Delta K$$

$$- A_e \sum_t \zeta_t^2 \ell_t (K+\Delta K) - D_0^J[(J+\Delta J)^2(J+\Delta J+1)^2 - J^2(J+1)^2]$$

$$- D_0^{JK}[(K+\Delta K)^2(J+\Delta J)(J+\Delta J+1) - K^2J(J+1)] - D_0^K[(K+\Delta K)^4 - K^4]$$

$$- \sum_s \alpha_s^B V_s (J+\Delta J)(J+\Delta J+1) - \sum_s (\alpha_s^A - \alpha_s^B) V_s (K+\Delta K)^2$$

where $\nu_0 = E_V - E_{V_0}$, J and K refer to the ground state, and ΔJ and ΔK are the difference between excited and ground state values.

IV.I. GROUND STATE COMBINATION DIFFERENCES

The general combination difference of two transitions in the same band is

$$ {}^{\Delta K_1}{}_{\Delta J_1}{}_{K_1}\, J_1 - {}^{\Delta K_2}{}_{\Delta J_2}{}_{K_2}\, J_2 \ . $$

For such a pair of transitions to have a common upper state and thus represent a genuine ground-state combination difference for axially symmetric molecules, it is necessary that $K_1 = K_2$, $\Delta K_1 = \Delta K_2$ and $J_1 + \Delta J_1 = J_2 + \Delta J_2$. The combination differences that satisfy these conditions are the following types:

$$ {}^{\Delta K}R_K(J-1) - {}^{\Delta K}P_K(J+1) $$

$$ {}^{\Delta K}R_K(J-1) - {}^{\Delta K}Q_K(J) $$

$$ {}^{\Delta K}Q_K(J) - {}^{\Delta K}P_K(J+1) $$

where ΔK may take on values -1, 0, +1.

All three types of ground state combination differences may be written in a form directly suitable for least squares fits, viz. (33)

$$ \begin{aligned} \text{GSCD}\ (\Delta J_1, \Delta J_2, K, J) &\equiv {}^{\Delta K}{}_{\Delta J_1}{}_{K}(J-J_1) - {}^{\Delta K}{}_{\Delta J_2}{}_{K}(J-\Delta J_2) \\ &= B_0(\Delta_2-\Delta_1) - D_0^J(\Delta_2^2-\Delta_1^2) + H_0^J(\Delta_2^3-\Delta_1^3) \\ &- D_0^{JK}(\Delta_2-\Delta_1)K^2 + H_0^{JK}(\Delta_2^2-\Delta_1^2)K^2 \\ &+ H_0^{KJ}(\Delta_2-\Delta_1)K^4 + \ldots \end{aligned} $$

where $\Delta_i = (J-\Delta J_i)(J+1-\Delta J_i)$, with i = 1 and 2, respectively.

In general, the ground-state combination differences are not affected by perturbations involving the upper levels of vibration-rotation transitions. But it is possible that a normally degenerate set of upper levels can be split by a perturbation and thus cause the various transitions, which in the absence of a perturbation would terminate on levels of same energy, would now terminate on two levels of different energy.

Examples of this are the lifting of the degeneracy of the $K = \ell = \pm 1$ levels in the upper state by Coriolis resonance or ℓ-type doubling (33).

CHAPTER V

THE $\nu_9 + \nu_{12}$ BAND OF C_2H_6

V.A. BACKGROUND

Ethane is one of the fundamental molecules of chemistry, the simplest containing the saturated carbon-carbon bond. Smith (34), and Hansen and Dennison (35) made extensive measurements under medium resolution. Allen, Plyler and Lafferty (36,37,38) analyzed a number of parallel bands of C_2H_6, C_2D_6, and $C^{13}C^{12}H_6$. They obtained good values of B_0, approximate values of D^J, D^{JK}, and r_o and r_s lengths for the C-C bond. Welsh (39-42) and co-workers have studied the Raman spectra of several vibration-rotation bands of C_2H_6, CD_3CH_3, and C_2D_6. In all cases, Welsh et al. have found perpendicular bands from which a value of A_0 can be obtained. Combining these values with previous infrared studies, a very complete structure for ethane has been derived.

Because of its molecular symmetry the ground state constants cannot be obtained from a microwave study. Cole and co-workers (43) have studied the ν_7 band of ethane under high resolution. They obtained an excellent value of B_0 and values of D_0^J and D_0^{JK}. Susskind (44,45) has studied the torsion-vibration-rotation interaction in ethane, and determined the barrier to internal rotation in ν_{11} and ν_{12}.

This work initially has the objective of studying the 1950-2550 cm^{-1} region of the ethane spectrum. A few bands had been assigned in this region by other studies (28). The spectra in this region are complicated

when observed under high resolution. In this work a perpendicular band centered near 2024 cm^{-1} has been assigned to the E_u component of $\nu_9 + \nu_{12}$ and a parallel band centered near 2008 cm^{-1} has been assigned to the A_{2u} component of $\nu_9 + \nu_{12}$. Approximately 700 transitions have been assigned in the perpendicular band and 300 transitions in the parallel band.

V.B. EXPERIMENT

The spectra are taken with 25 Torr pressure of C_2H_6 in a 12 m path at ambient temperature. The C_2H_6 sample is obtained from Matheson Gas Products and is stated to be 99.9% pure. The spectra are recorded using the five meter Littrow instrument. A Bausch and Lomb 20 cm x 40 cm, 31.6 groove/mm grating is used in the eleventh and twelfth orders to cover the entire band. The slit width is varied during the scans to keep the recorded signal level high. The data are recorded digitally at a rate of approximately 2.5 cm^{-1}/hr. A NaCl prism is used to sort out the grating orders. The detector, InSb, which is made by Santa Barbara Research Center, is cooled by liquid nitrogen. The resolution of the spectra is about 0.020 cm^{-1}. The maximum absorption for an isolated line is about 50%.

V.C. CALIBRATION

Some amount of CO is added to the sample cell and calibration is accomplished by using the 1←0 carbon monoxide band occurring in the eleventh and twelfth orders. All the CO lines that are present in the

same region as the $\nu_9 + \nu_{12}$ band are used in calibration. The calibration lines in the 1940-2033 cm^{-1} region are inserted by changing grating orders. To calibrate the scans without CO lines, one well-shaped C_2H_6 line on each side of a CO line in the calibrated scans is identified and used as a reference line. Let X_C denote the line position of the CO line and X_L and X_H denote the line positions of the C_2H_6 lines. If Y_L and Y_H are the line positions of the corresponding C_2H_6 lines in the scan without CO lines, then the CO line is assumed to appear at $(X_C-X_L)\frac{Y_H-Y_L}{X_H-X_L} + Y_L$ in the scans without CO lines. This method will yield good results as long as the reference lines are close together.

V.D. MEASUREMENT AND WEIGHTING

The spectra are measured automatically by a program named "PEKFIN," which is adopted from "Savitzky Peakfinder" program (46). All lines with moderate absorptions are measured and stored in an output file, which can be used as input for further computation.

Each line is weighted between 0.0 and 9.0 by inspection on the basis of estimated measurement accuracy which is judged from the line shape and signal to noise ratio.

V.E. ASSIGNMENT

The spectra of $\nu_9 + \nu_{12}$ are complicated in the 1940-2050 cm^{-1} region due to the overlapping of the perpendicular and parallel bands. Many Loomis-Wood diagrams (47) are produced and used in the identification of series of lines in the spectra. In the perpendicular band,

individual lines are assigned in the subbands with $K\Delta K$ = 12 to -7 and corresponding Q-branches. In the parallel band, individual lines are assigned in the subbands with K = 0 to 7. All the P_P and P_R series in the perpendicular band are relatively weak and have not been assigned. Figure V.1 shows one section of the spectrum where parallel and perpendicular bands overlap with each other. Figure V.2 shows one section of the perpendicular band. Tables V.1-V.6 give listings of the assigned lines of $\nu_9 + \nu_{12}$.

V.F. GROUND STATE PARAMETERS FROM MEASURED COMBINATION DIFFERENCES

The procedures described by Blass and Edwards (33) are used to find the ground state parameters B_0, D_0^J, D_0^{JK}, by using 410 properly weighted GSCD's (ground state combination differences). A least-squares regression analysis program is used to fit the GSCD's to the expression given in (33). The program is allowed to delete GSCD's with weighted residuals greater than 0.015 cm^{-1} and omit insignificant terms from the regression model. The standard deviation of the fit is .0044 cm^{-1}. The resulting ground state parameters are given in Table V.7. For comparison, results of previous work on this molecule by Allen, Plyler and Lafferty (36,37) and by Cole et al. (43) are listed in Table V.8.

V.G. MOLECULAR PARAMETERS FOR THE PERPENDICULAR BAND OF $\nu_9 + \nu_{12}$

In the perpendicular band, $^RR_0$, $^RQ_0$ and all the ^PP, ^PQ branches are found to be perturbed, and they are excluded from the fit in obtaining

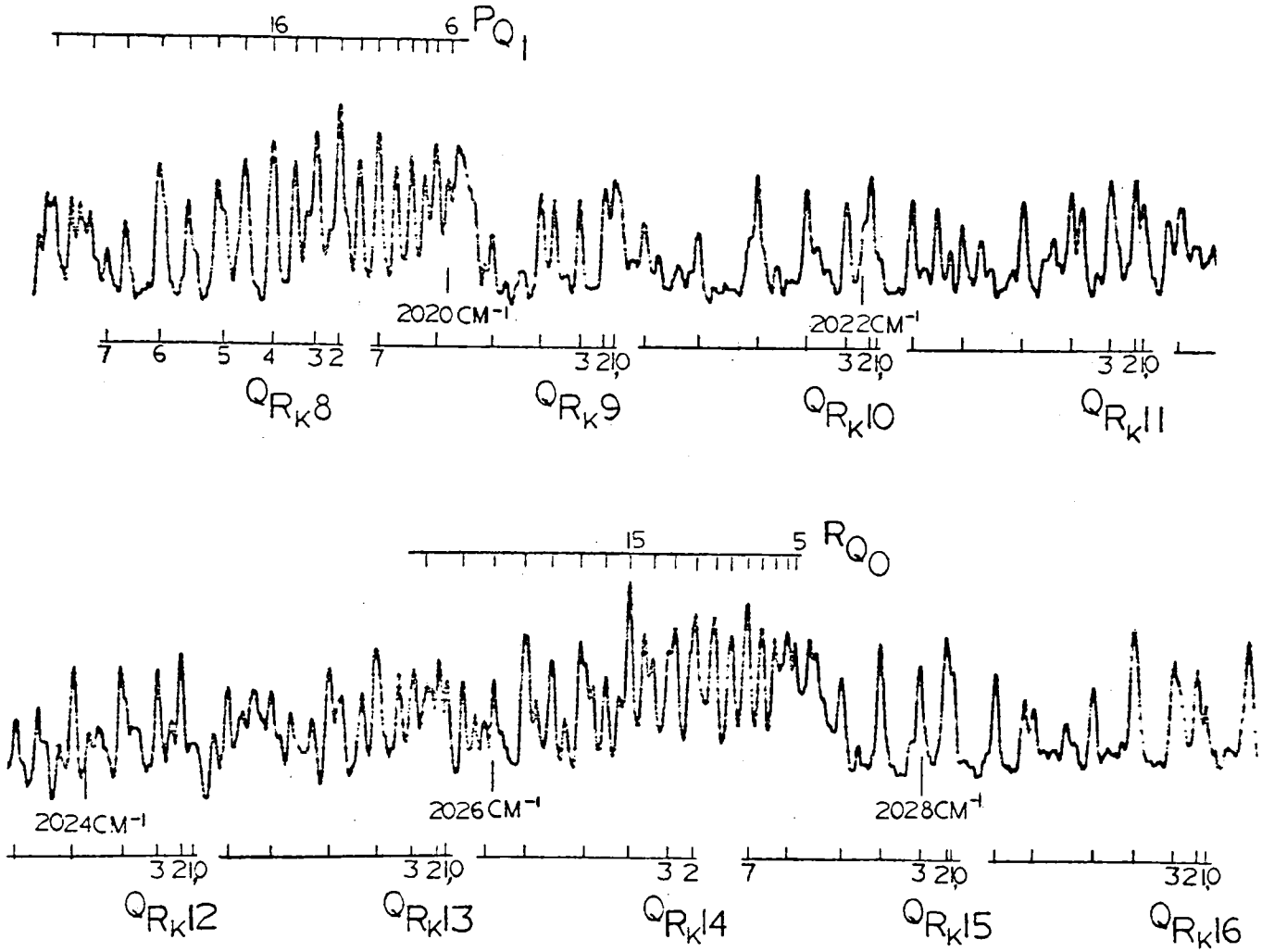


Figure V.1. Spectra of C_2H_6 from 2018 to 2029 cm^{-1}.

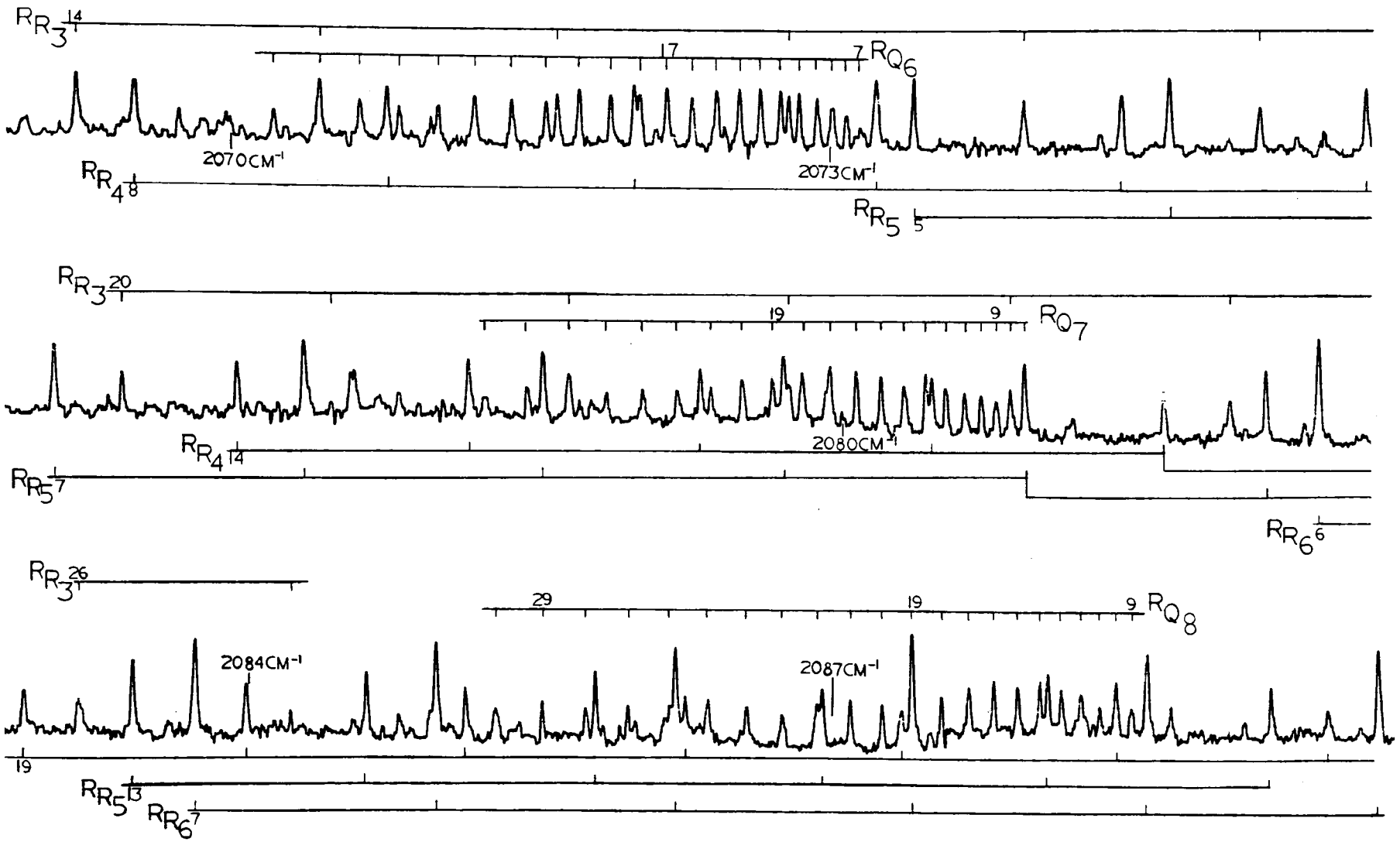


Figure V.2. Spectra of C_2H_6 from 2069 to 2090 cm^{-1}.

TABLE V.1

OBSERVED $^{Q}R_{K}(J)$ TRANSITIONS OF $\nu_9 + \nu_{12}$

J	K=0, 1	2	3	4	5	6	7
2	2011.9160	2011.8623	0.0000	0.0000	0.0000	0.0000	0.0000
3	2013.2061	2013.1621	2013.0377	0.0000	0.0000	0.0000	0.0000
4	0.0000	2014.4506	2014.3306	2014.1443	0.0000	0.0000	0.0000
5	2015.7731	2015.7336	2015.6108	2015.4358	2015.1977	0.0000	0.0000
6	2017.0463	2017.0110	2016.8904	2016.7104	2016.4703	2016.1913	0.0000
7	2018.3193	2018.2787	2018.1628	2017.9817	2017.7407	2017.4584	2017.1624
8	0.0000	2019.5412	2019.4355	2019.2319	0.0000	2018.6887	2018.4467
9	2020.8396	2020.7940	2020.6777	2020.4908	2020.2567	2019.9906	2019.7184
10	0.0000	2022.0407	2021.9246	2021.7349	2021.5037	0.0000	2020.9765
11	2023.3154	2023.2773	2023.1625	2022.9755	2022.7497	2022.4662	2022.2299
12	2024.5503	2024.5043	2024.3920	2024.2066	2023.9802	2023.7031	2023.4813
13	2025.7723	2025.7312	2025.6139	2025.4242	2025.2051	2024.9318	2024.7241
14	0.0000	2026.9564	2026.8293	2026.6437	2026.4310	2026.1461	2025.9471
15	2028.1935	2028.1588	2028.0367	2027.8493	2027.6550	2027.3683	2027.2018
16	2029.3960	2029.3564	2029.2435	2029.0484	2028.8588	2028.5731	2028.3946
17	2030.5909	2030.5464	2030.4306	2030.2340	2030.0585	2029.7826	2029.6042
18	0.0000	2031.7357	2031.6109	2031.4090	2031.2560	2030.9674	2030.8023
19	2032.9558	2032.9126	2032.7815	2032.5808	2032.4485	2032.1548	2032.0066
20	0.0000	2034.0649	0.0000	2033.7467	2033.6317	2033.3252	0.0000
21	2035.2852	2035.2436	2035.1160	2034.8822	2034.8193	2034.4998	0.0000
22	2036.4446	2036.3929	2036.2653	2036.0431	2035.9699	2035.6570	0.0000
23	2037.5693	0.0000	2037.4072	0.0000	2037.1376	0.0000	0.0000
24	0.0000	2038.6793	2038.5434	0.0000	0.0000	0.0000	0.0000
25	0.0000	2039.8036	0.0000	0.0000	2039.4573	0.0000	0.0000
26	0.0000	0.0000	0.0000	0.0000	2040.5608	0.0000	0.0000
27	0.0000	0.0000	0.0000	0.0000	2041.7491	0.0000	0.0000
28	0.0000	0.0000	0.0000	0.0000	2042.8961	0.0000	0.0000

TABLE V.2

OBSERVED $^{Q}P_{K}(J)$ TRANSITIONS OF $\nu_9 + \nu_{12}$

J	K=0, 1	2	3	4	5	6	7
1	2006.6351	0.0000	0.0000	0.0000	0.0000	0.0000	0.0000
2	2005.3045	0.0000	0.0000	0.0000	0.0000	0.0000	0.0000
3	2003.9562	2003.9266	0.0000	0.0000	0.0000	0.0000	0.0000
4	0.0000	2002.5949	2002.4540	0.0000	0.0000	0.0000	0.0000
5	2001.2544	2001.2114	2001.1049	2000.9199	0.0000	0.0000	0.0000
6	0.0000	1999.8621	1999.7444	1999.5659	1999.3183	0.0000	0.0000
7	1998.5325	1998.4953	1998.3767	1998.1890	1997.9522	1997.6731	0.0000
8	0.0000	1997.1200	1997.0022	1996.8141	1996.5819	1996.2974	1995.9924
9	1995.7727	1995.7386	1995.6208	1995.4349	1995.2084	1994.9157	0.0000
10	1994.3839	1994.3588	1994.2316	1994.0480	1993.8068	1993.5329	1993.2572
11	1992.9933	1992.9524	1992.8365	1992.6514	1992.4203	1992.1379	1991.8868
12	1991.5896	1991.5483	1991.4312	1991.2496	1991.0171	1990.7390	1990.4888
13	1990.1812	1990.1400	1990.0215	1989.8395	1989.6117	1989.3342	1989.0938
14	1988.7858	1988.7221	1988.6072	1988.4241	1988.2053	1987.9232	1987.6972
15	1987.3477	1987.3026	1987.1841	1986.9985	1986.7875	1986.5077	1986.2943
16	1985.9142	1985.8689	1985.7472	1985.5678	1985.3630	1985.0846	1984.8796
17	1984.4740	1984.4339	1984.3173	1984.1298	1983.9324	1983.6467	1983.4585
18	0.0000	1982.9931	1982.8747	1982.6804	1982.4976	1982.2145	1982.0321
19	1981.5832	1981.5420	1981.4181	1981.2256	1981.0466	1980.7753	1980.5931
20	1980.1267	1980.0778	1979.9462	1979.7651	1979.6092	1979.3255	1979.1618
21	1978.6590	1978.6163	1978.5008	1978.2997	1978.1519	1977.8696	1977.7133
22	0.0000	1977.1445	1977.0181	1976.8151	1976.6986	1976.4018	1976.2635
23	1975.7080	1975.6662	1975.5420	1975.3409	1975.2304	1974.9387	0.0000
24	1974.2281	0.0000	1974.0584	1973.8966	1973.7502	1973.4621	1973.3469
25	0.0000	0.0000	1972.5592	0.0000	1972.2902	0.0000	1971.8888
26	0.0000	0.0000	0.0000	0.0000	1970.8093	0.0000	0.0000
27	0.0000	0.0000	0.0000	0.0000	1969.3273	0.0000	0.0000
28	0.0000	0.0000	0.0000	0.0000	1967.8278	0.0000	0.0000

TABLE V.3

OBSERVED $^{P}Q_{K}(J)$ TRANSITIONS OF $\nu_9 + \nu_{12}$

J	K=1	2	3	4	5	6	7
3	0.0000	0.0000	2006.9540	0.0000	0.0000	0.0000	0.0000
4	0.0000	0.0000	0.0000	0.0000	0.0000	0.0000	0.0000
5	0.0000	0.0000	0.0000	0.0000	0.0000	0.0000	0.0000
6	2020.0479	2012.9840	2005.9731	1996.3838	0.0000	0.0000	0.0000
7	2019.9907	2012.9436	2005.9396	1996.3425	1989.1816	0.0000	0.0000
8	2019.9377	2012.8937	2005.8941	1996.2974	1989.1377	0.0000	0.0000
9	2019.8738	2012.8393	2005.8591	1996.2474	1989.0938	0.0000	0.0000
10	2019.7992	2012.7717	2005.7993	1996.1884	1989.0392	1981.3784	1973.9616
11	2019.7184	2012.7069	2005.7343	1996.1305	1988.9807	1981.3021	1973.8962
12	2019.6336	2012.6389	2005.6819	1996.0613	1988.9149	1981.2256	1973.8271
13	2019.5412	2012.5602	2005.6155	1995.9924	1988.8560	1981.1367	1973.7517
14	2019.4355	2012.4650	2005.5502	1995.9096	1988.7858	1981.0466	1973.6595
15	2019.3336	2012.3749	2005.4590	1995.8294	1988.7221	1980.9398	1973.5686
16	2019.2319	2012.2688	2005.3838	1995.7387	1988.6516	1980.8366	0.0000
17	2019.0993	2012.1582	2005.3046	1995.6382	0.0000	0.0000	0.0000
18	2018.9685	2012.0403	2005.2184	1995.5398	0.0000	0.0000	0.0000
19	2018.8285	2011.9181	2005.1293	1995.4349	0.0000	0.0000	0.0000
20	2018.6888	2011.7875	0.0000	1995.3302	0.0000	0.0000	0.0000
21	2018.5312	2011.6559	2004.9243	1995.2084	0.0000	0.0000	0.0000
22	2018.3665	0.0000	0.0000	1995.1004	0.0000	0.0000	0.0000
23	2018.1959	0.0000	2004.6928	1994.9786	0.0000	0.0000	0.0000
24	2018.0277	0.0000	2004.5887	1994.8449	0.0000	0.0000	0.0000
25	2017.8445	0.0000	2004.4704	1994.7160	0.0000	0.0000	0.0000

TABLE V.4

OBSERVED $^{P}P_{K}(J)$ TRANSITIONS OF $\nu_9 + \nu_{12}$

J	K=1	2	3	4	5	6	7
2	2017.5273	2010.4636	0.0000	0.0000	0.0000	0.0000	0.0000
3	2016.1916	0.0000	2002.0855	0.0000	0.0000	0.0000	0.0000
4	2014.8361	2007.7769	2000.7469	0.0000	0.0000	0.0000	0.0000
5	2013.4858	2006.4225	1999.3978	0.0000	1982.6516	0.0000	0.0000
6	2012.1225	2005.0500	1998.0473	1988.4589	1981.3021	1973.7013	0.0000
7	2010.7586	2003.7079	1996.6898	1987.1019	1979.9480	1972.3372	1964.8679
8	2009.3839	2002.3424	1995.3302	1985.7472	1978.5787	1970.9669	1963.5075
9	2008.0006	0.0000	1993.9626	1984.3733	1977.2135	1969.5833	1962.1389
10	2006.6085	1999.5661	1992.5910	1982.9931	1975.8380	1968.1976	1960.7652
11	2005.2184	1998.1890	0.0000	1981.6146	1974.4612	1966.8052	1959.3832
12	2003.8119	1996.8141	1989.8395	1980.2269	1973.0834	1965.4035	1957.9952
13	2002.4042	1995.4063	1988.4589	1978.8372	1971.7032	1964.0007	1956.5988
14	2000.9844	0.0000	1987.0591	1977.4409	1970.3094	1962.5863	1955.1958
15	1999.5661	1952.5910	1985.6708	1976.0403	1968.9165	1961.1665	1953.7851
16	1998.1302	1991.1653	1984.2742	1974.6369	1967.5259	1959.7427	1952.3684
17	1996.6858	1989.7447	1982.8747	1973.2266	1966.1349	1958.3091	1950.9473
18	1995.2451	1988.3141	0.0000	1971.8073	1964.7363	1956.8690	1949.5120
19	1993.8068	1986.8853	0.0000	1970.3855	1963.3411	1955.4236	0.0000
20	1992.3375	1985.4352	1978.6589	1968.9607	1961.9452	1953.9711	1946.6282
21	1990.8717	1983.9844	1977.2139	1967.5259	1960.5290	1952.5131	0.0000
22	1989.3546	0.0000	0.0000	1966.0939	1959.1372	1951.0478	1943.7259
23	1987.9231	1981.0467	1974.3894	1964.6547	0.0000	1949.5764	1942.2595
24	0.0000	0.0000	0.0000	1963.2140	0.0000	0.0000	1940.7814
25	0.0000	0.0000	1971.5198	1961.7692	0.0000	0.0000	0.0000
26	0.0000	0.0000	1970.0712	1960.3135	0.0000	0.0000	0.0000
27	0.0000	0.0000	1968.6178	1958.8624	0.0000	0.0000	0.0000
28	0.0000	0.0000	0.0000	1957.3942	0.0000	0.0000	0.0000

TABLE V.5

OBSERVED $^{R}Q_{K}(J)$ TRANSITIONS OF $\nu_9 + \nu_{12}$

J	K=Ø	1	2	3	4	5	6
4	2027.5013	2035.0157	2042.5913	0.0000	0.0000	0.0000	0.0000
5	2027.4304	2034.9801	2042.5523	0.0000	0.0000	0.0000	0.0000
6	2027.3923	2034.9304	2042.5124	2050.1252	0.0000	2065.4885	0.0000
7	2027.3340	2034.8819	2042.4552	2050.0737	2057.7353	2065.4356	2073.1753
8	2027.2728	2034.8184	2042.3968	2050.0091	2057.6719	2065.3743	2073.1090
9	2027.2026	2034.7529	2042.3266	2049.9387	2057.6059	2065.3051	2073.0375
10	2027.1205	2034.6784	2042.2525	2049.8619	2057.5265	2065.2210	2072.9614
11	2027.0447	2034.5928	2042.1672	2049.7782	2057.4381	2065.1421	2072.8741
12	2026.9550	2034.5035	2042.0773	2049.6878	2057.3438	2065.0482	2072.7801
13	2026.8616	2034.4017	2041.9779	2049.5907	2057.2460	2064.9467	2072.6779
14	2026.7543	2034.2974	2041.8706	2049.4846	2057.1397	2064.8426	2072.5706
15	2026.6428	2034.1817	2041.7511	2049.3680	2057.0255	2064.7215	2072.4531
16	2026.5307	2034.0654	0.0000	2049.2424	2056.9026	2064.5972	2072.3268
17	2026.4086	2033.9283	2041.5003	2049.1110	2056.7626	2064.4680	2072.1952
18	2026.2729	2033.7833	2041.3654	2048.9745	2056.6282	2064.3273	2072.0516
19	2026.1461	2033.6336	2041.2175	2048.8292	2056.4808	2064.1788	2071.9062
20	2025.9959	2033.4812	2041.0644	2048.6770	2056.3291	2064.0248	2071.7467
21	2025.8465	2033.3249	2040.9054	2048.5113	2056.1665	2063.8617	2071.5856
22	2025.6708	0.0000	2040.7319	2048.3424	2055.9923	2063.6905	2071.4145
23	0.0000	0.0000	0.0000	2048.1677	2055.8130	2063.5105	2071.2300
24	0.0000	0.0000	0.0000	2047.9811	2055.6313	2063.3201	2071.0460
25	0.0000	0.0000	0.0000	2047.8093	2055.4375	2063.1264	2070.8491
26	0.0000	0.0000	0.0000	2047.5795	0.0000	2062.9258	2070.6447
27	0.0000	0.0000	0.0000	2047.3796	0.0000	2062.7151	2070.4428
28	0.0000	0.0000	0.0000	2047.1611	0.0000	2062.5011	0.0000
29	0.0000	0.0000	0.0000	2046.9338	0.0000	0.0000	0.0000
30	0.0000	0.0000	0.0000	2046.6878	0.0000	0.0000	0.0000
31	0.0000	0.0000	0.0000	2046.4627	0.0000	0.0000	0.0000
32	0.0000	0.0000	0.0000	2046.2123	0.0000	0.0000	0.0000
33	0.0000	0.0000	0.0000	2045.9630	0.0000	0.0000	0.0000

TABLE V.5 (continued)

J	K=7	8	9	10	11	12
8	2080.8769	0.0000	0.0000	0.0000	0.0000	0.0000
9	2080.8025	2088.5995	0.0000	0.0000	0.0000	0.0000
10	2080.7263	2088.5206	2096.3489	0.0000	0.0000	0.0000
11	2080.6427	2088.4356	2096.2610	2104.1084	0.0000	0.0000
12	2080.5469	2088.3436	2096.1660	0.0000	0.0000	0.0000
13	2080.4446	2088.2403	2096.0635	0.0000	0.0000	0.0000
14	2080.3356	2088.1291	2095.9507	2103.8094	2111.6857	2119.6065
15	2080.2161	2088.0081	2095.8332	2103.6870	0.0000	2119.4713
16	2080.0916	2087.8838	2095.7078	2103.5548	2111.4440	2119.3498
17	2079.9577	2087.7509	2095.5725	2103.4192	2111.3006	2119.2122
18	2079.8162	2087.6067	2095.4266	2103.2750	2111.1566	2119.0628
19	2079.6659	2087.4519	2095.2772	2103.1229	2111.0017	2118.9081
20	2079.5101	2087.2979	2095.1196	2102.9630	2110.8392	2118.7497
21	2079.3467	2087.1337	2094.9515	2102.8003	2110.6707	2118.5737
22	2079.1739	2086.9574	2094.7759	2102.6210	2110.4918	2118.3944
23	2078.9903	2086.7754	2094.5935	2102.4328	2110.3109	2118.2116
24	2078.8051	2086.5860	2094.4018	2102.2417	2110.1133	2118.0064
25	2078.6114	2086.3844	2094.2030	2102.0401	2109.9106	0.0000
26	2078.3991	2086.2129	0.0000	0.0000	0.0000	0.0000
27	2078.1877	2085.9657	0.0000	0.0000	0.0000	0.0000
28	2077.9680	2085.7437	0.0000	0.0000	0.0000	0.0000
29	0.0000	2085.5182	0.0000	0.0000	0.0000	0.0000
30	0.0000	2085.2836	0.0000	0.0000	0.0000	0.0000

TABLE V.6

OBSERVED $^{R}R_{K}(J)$ TRANSITIONS OF $\nu_9 + \nu_{12}$

J	K=Ø	1	2	3	4	5	6
0	2028.8558	0.0000	0.0000	0.0000	0.0000	0.0000	0.0000
1	2030.1753	0.0000	0.0000	0.0000	0.0000	0.0000	0.0000
2	2031.4565	2039.0223	2046.6007	0.0000	0.0000	0.0000	0.0000
3	2032.7009	2040.3210	2047.8991	2055.5013	0.0000	0.0000	0.0000
4	2034.0654	0.0000	2049.1765	2056.8086	2064.4682	0.0000	0.0000
5	2035.3544	2042.8961	2050.4651	2058.0843	2065.7489	2073.4452	0.0000
6	2036.6317	0.0000	2051.7368	2059.3566	2067.0161	2074.7163	2082.4487
7	2037.9001	2045.4157	2052.9969	2060.6177	2068.2817	2075.9780	2083.7116
8	2039.1609	2046.6874	2054.2530	2061.8738	2069.5361	2077.2353	2084.9677
9	2040.4179	2047.9263	2055.5013	2063.1261	2070.7856	2078.4816	2086.2129
10	0.0000	2049.1765	0.0000	2064.3613	2072.0239	2079.7208	2087.4519
11	2042.8961	2050.4096	2057.9817	2065.5990	2073.2573	2080.9515	2088.6824
12	2044.1529	2051.6351	2059.2123	2066.8199	2074.4796	2082.1754	2089.9049
13	2045.3628	2052.8414	2060.4257	2068.0366	2075.6966	2083.3904	2091.1205
14	2046.6007	2054.0483	2061.6362	2069.2471	2076.9013	2084.5963	2092.3238
15	0.0000	2055.2515	2062.8342	2070.4428	2078.1006	2085.7939	2093.5209
16	0.0000	0.0000	2064.0241	2071.6371	2079.2919	2086.9852	2094.7104
17	2050.2253	2057.6089	2065.2227	2072.8199	2080.4748	2088.1676	2095.8924
18	2051.4270	2058.8110	2066.3864	2074.0001	2081.6483	2089.3431	2097.0647
19	2052.6189	2059.9734	2067.5544	2075.1673	2082.8161	2090.5102	2098.2287
20	2053.8004	2061.1330	2068.7170	2076.3235	2083.9737	2091.6651	2099.3845
21	2055.0040	2062.2760	0.0000	0.0000	2085.1227	2092.8147	2100.5294
22	2056.1139	2063.4136	2071.0077	2078.6114	2086.2627	2093.9573	2101.6731
23	2057.3458	2064.5506	2072.1358	2079.7460	2087.3981	2095.0881	2102.8003
24	2058.5114	0.0000	0.0000	2080.8769	2088.5206	2096.2090	2103.9236
25	2059.6670	0.0000	0.0000	2081.9874	2089.6372	2097.3275	2105.0423
26	2060.8282	0.0000	0.0000	2083.1009	2090.7470	2098.4319	2106.1500
27	2062.0369	0.0000	0.0000	2084.2012	0.0000	2099.5336	2107.2465
28	2063.1261	0.0000	0.0000	0.0000	0.0000	0.0000	2108.3341

TABLE V.6 (continued)

J	K=7	8	9	10	11	12
6	0.0000	0.0000	0.0000	0.0000	0.0000	0.0000
7	2091.4799	0.0000	0.0000	0.0000	0.0000	0.0000
8	2092.7345	0.0000	0.0000	0.0000	0.0000	0.0000
9	2093.9795	2101.7738	2109.6902	0.0000	0.0000	0.0000
10	2095.2168	2103.0106	2110.8392	2118.6973	0.0000	0.0000
11	2096.4464	2104.2408	2112.0690	2119.9241	2127.8068	0.0000
12	2097.6686	2105.4627	2113.2890	2121.1434	2129.0260	2136.9352
13	2098.8803	2106.6761	2114.5020	2122.3543	2130.2361	2138.1423
14	2100.0870	2107.8798	2115.7063	2123.5564	2131.4400	2139.3423
15	2101.2842	2109.0754	2116.9024	2124.7499	2132.6323	2140.5350
16	2102.4735	2110.2650	2118.0876	2125.9353	2133.8184	2141.7193
17	2103.6544	2111.4440	2119.2664	2127.1142	2134.9929	2142.8969
18	2104.8262	2112.6154	2120.4370	2128.2830	2136.1567	2144.0581
19	2105.9881	2113.7780	2121.5964	2129.4458	2137.3194	2145.2172
20	2107.1457	2114.9326	2122.7524	2130.5968	2138.4693	2146.3660
21	2108.2897	2116.0791	2123.8995	2131.7367	2139.6118	2147.5056
22	2109.4281	2117.2163	2125.0352	2132.8703	2140.7418	2148.6339
23	2110.5626	2118.3448	2126.1641	2134.0000	2141.8661	2149.7541
24	2111.6857	2119.4713	2127.2831	2135.1180	2142.9869	0.0000
25	2112.7982	2120.5813	2128.3968	2136.2243	2144.0969	0.0000
26	2113.9040	2121.6786	2129.4983	0.0000	0.0000	0.0000
27	2114.9982	0.0000	0.0000	2138.4213	0.0000	0.0000
28	0.0000	2123.8655	0.0000	0.0000	0.0000	0.0000
29	0.0000	0.0000	0.0000	0.0000	0.0000	0.0000
30	0.0000	2126.0055	0.0000	0.0000	0.0000	0.0000

TABLE V.7

GROUND STATE PARAMETERS FOR C_2H_6[a]

B_0	$0.66308141(\pm\ 0.190 \times 10^{-4})\,cm^{-1}$
D_0^J	$1.134 \times 10^{-6}(\pm\ 0.272 \times 10^{-7})\,cm^{-1}$
D_0^{JK}	$2.396 \times 10^{-6}(\pm\ 0.427 \times 10^{-6})\,cm^{-1}$

TABLE V.8

RESULTS OF PREVIOUS STUDIES

Band	$B_0(cm^{-1})$	$D_0^J(cm^{-1})$	$D_0^{JK}(cm^{-1})$
ν_7[a]	0.663135 ± 0.000048	$(1.18 \pm 0.07)x10^{-6}$	$(3.6 \pm 1.2)x10^{-6}$
$\nu_2+\nu_6$[b]	0.66310 ± 0.00007	$(7 \pm 2)x10^{-7}$	$(6 \pm 3)x10^{-6}$
$\nu_2+\nu_6$[c]	0.6537	-2.2×10^{-6}	9×10^{-6}

[a] A. R. H. Cole et al. (43).

[b] W. J. Lafferty et al. (37).

[c] H. C. Allen et al. (36).

the molecular parameters for the perpendicular band of $\nu_9 + \nu_{12}$. A least-squares regression analysis is performed on the observed 440 transitions in the $^{R}R_K$ and $^{R}Q_K$ branches with K = 1 to 12. The standard deviation of the fit is 0.0033 cm^{-1}. Table V.9 lists the determined molecular parameters for the perpendicular band of $\nu_9 + \nu_{12}$.

V.H. PERTURBATIONS

The zero subband, which consists of transitions terminating on the $K = \ell = \pm 1$ upper state levels, exhibits ℓ-type doubling and has been treated by using the relation

$$[^{R}R_o(J-1) - {}^{R}Q_o(J)]_{exp} = [^{R}R_o(J-1) - {}^{R}Q_o(J)]_{cal} + qJ(J+1)$$

where $[^{R}R_o(J-1) - {}^{R}Q_o(J)]_{cal}$ is calculated using the ground state constants obtained in this study. A least-squares fit gives $q_{9+12} = -0.323 \times 10^{-3}(\pm\ 0.23 \times 10^{-4})$ cm^{-1} with the standard deviation of the fit equal to 5.3×10^{-3} cm^{-1}.

When the following equations (33),

$$[^{R}R_o(J)]_{exp} = [^{R}R_o(J)]_{cal} + [\beta + \frac{(\alpha')^2}{\sigma}]J(J+1)$$

$$[^{R}Q_o(J)]_{exp} = [^{R}Q_o(J)]_{cal} - \beta J(J+1)$$

are used to fit the observed $^{R}R_o$ and $^{R}Q_o$ transitions, the fits are poor and residuals of the fit indicate there are still other types of perturbations involved.

TABLE V.9

MOLECULE PARAMETERS FOR THE E_u BAND OF $\nu_9 + \nu_{12}$[a]

$\nu_0 - A_e \zeta^z_{9+12}$	2023.7945 cm^{-1}
$A_0 - B_0 + A_e \zeta^z_{9+12}$	3.7347181 ± 0.00010 cm^{-1}
$D^K_0 - \frac{1}{4} \eta_K$	(7.9843616 ± 0.030)x10^{-5} cm^{-1}
$\alpha^A_{9+12} - \alpha^B_{9+12}$	(-2.3085005 ± 0.0014)x10^{-2} cm^{-1}
α^B_{9+12}	(3.7692831 ± 0.0033)x10^{-3} cm^{-1}
η_J	(-1.5835645 ± 0.035)x10^{-5} cm^{-1}

[a]Error limits given correspond to a 95% confidence interval.

The parallel band is found also to be perturbed. No subset of unperturbed lines have been definitely identified.

Figure V.3 is a plot of residuals, i.e., Δ_{oc}'s [$\Delta_{oc} = \nu_{obs} - \nu_{calc}$] for most of the perturbed $^{P}P_{K}(J)$ transitions.

Figure V.4 is a plot of residuals for $^{R}R_{o}(J)$ and $^{R}Q_{o}(J)$. The patterns in Figure V.3 do not seem to be complicated. The perturbations are likely to be the results of interactions involving 2 or 3 states. From perturbation theory, the summation of the deviations of the interacting states is equal to zero. From Figure V.3, the relative deviation of $^{P}P_{3}$ and $^{P}P_{4}$ subbands are about 2 cm^{-1}. Judging from the structure of the K-lines in each J-group in the parallel band, the relative deviations in the A_{2u} component are believed to be well within 1 cm^{-1}. The possibility of explaining the observed perturbations as the result of the interaction between A_{2u} and E_{u} bands is thus assumed to be unlikely. Further research is required if these perturbations are to be explained. Investigation of $\nu_{9} + \nu_{12}$ of $C_{2}D_{6}$ may be particularly helpful.

V.I. CONCLUSIONS

The ground state parameters determined from combination differences are consistent and slightly better than those obtained by Cole et al. (43). The molecular parameters determined here for $\nu_{9} + \nu_{12}$ should be combined with future studies of this molecule at high resolution to determine more accurate Coriolis coupling constants and other anharmonicity constants of ethane.

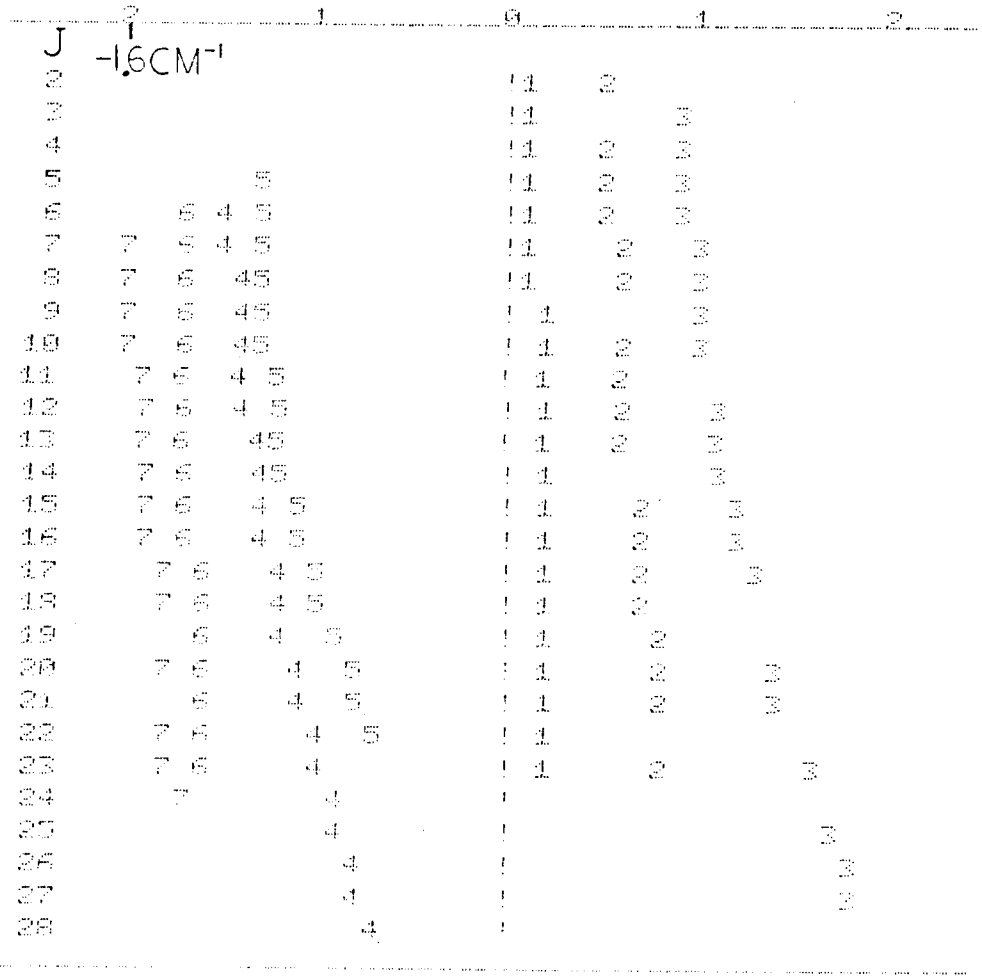


Figure V.3. (Observed Wavenumbers) — (Calculated Wavenumbers) for $P_{P_K}(J)$.

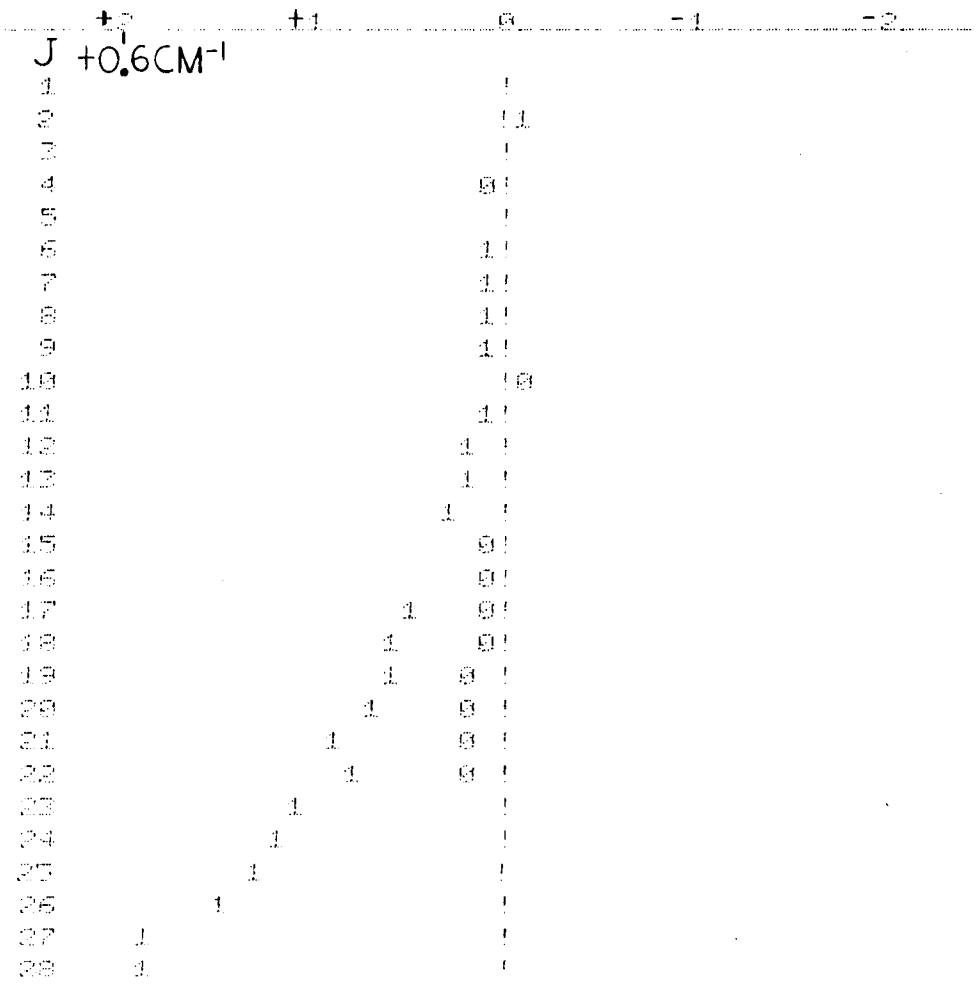


Figure V.4. (Observed Wavenumbers) — (Calculated Wavenumbers) for $^{R}R_{o}(J)$ and $^{R}Q_{o}(J)$.

REFERENCES

REFERENCES

1. D. E. Jennings, Thesis, University of Tennessee (1974).

2. K. N. Rao, C. J. Humphreys, D. H. Rank, Wavelength Standards in the Infrared, Academic, New York (1966).

3. N. R. Draper and H. Smith, Applied Regression Analysis, Wiley & Sons, New York (1966).

4. C. Daniel and F. S. Wood, Fitting Equations to Data, Wiley-Interscience, New York (1971).

5. R. P. Feyman, R. B. Leighton and M. Sands, Lectures on Physics, Vol. 1, Addison-Wesley, New York, 6-5 (1966).

6. F. Reif, Fundamentals of Statistical and Thermal Physics, McGraw-Hill, New York (1965).

7. G. Guelachvili, Optics Communications 8, 171 (July 1973).

8. G. Guelachvili, AMCO V, Paris, Plenum Press (June 1975).

9. M. Kurlat, Thesis, University of Tennessee (1969).

10. J. A. Hafford, Thesis, University of Tennessee (1972).

11. H. H. Nielsen, Handbuch per Physics 37, 1 (1959).

12. E. B. Wilson, Jr., and J. B. Howard, J. Chem. Phys. 4, 260 (1936).

13. H. C. Allen and P. C. Cross, Molecular Vib-Rotors, Wiley & Sons, New York (1963).

14. M. Born and R. Oppenheimer, Ann. Physik 84, 457 (1927).

15. B. T. Darling and D. M. Dennison, Phys. Rev. 57, 128 (1940).

16. J. K. G. Watson, Mol. Phys. 15, 479 (1968).

17. M. Goldsmith, G. Amat, and H. H. Nielsen, J. Chem. Phys. 24, 1178 (1956).

18. G. Amat, M. Goldsmith, and H. H. Nielsen, J. Chem. Phys. 27, 838 (1957).

19. G. Amat and H. H. Nielsen, J. Chem. Phys. 27 845 (1957).

20. G. Amat and H. H. Nielsen, J. Chem. Phys. 29, 665 (1958).

21. G. Amat and H. H. Nielsen, J. Chem. Phys. 34, 339 (1961).

22. G. Amat and H. H. Nielsen, J. Chem. Phys. 36, 1859 (1962).

23. G. Tarrago, Cahiers Phys. 19, 149 (1965).

24. S. Maes, J. Mol. Spectry. 9, 204 (1962).

25. W. E. Blass and A. H. Nielsen, Methods of Experimental Physics, L. Marton, ed., 3A, Academic, New York (1974).

26. G. Amat, H. H. Nielsen, and G. Tarrago, Rotation-Vibration of Polyatomic Molecules, Dekker, New York (1971).

27. W. E. Blass, Thesis, Michigan State University (1963).

28. G. Herzberg, Infrared and Raman Spectra of Polyatomic Molecules, D. Van Nostrand Co., New York (1945).

29. J. Overrend, Vibrational Spectra and Structure, J. R. Durig, ed., Vol. 3, Dekker, New York (1975).

30. J. T. Hougen, J. Chem. Phys. 37, 1433 (1962).

31. H. C. Longuet-Higgins, Mol. Phys. 6, 445 (1963).

32. W. E. Blass, J. Mol. Spectry. 31, 196 (1969).

33. W. E. Blass and T. H. Edwards, J. Mol. Spectry. 24, 111 (1967).

34. L. G. Smith, J. Chem. Phys. 17, 139 (1949).

35. G. E. Hansen and D. M. Dennison, J. Chem. Phys. 20, 313 (1952).

36. H. C. Allen and E. K. Plyler, J. Chem. Phys. 31, 1062 (1959).

37. W. J. Lafferty and E. K. Plyler, J. Chem. Phys. 37, 2688 (1962).

38. W. J. Lafferty and E. K. Plyler, J. Res. Natl. Bur. Std., A67, 225 (1963).

39. J. Romanko, T. Feldman, and H. L. Welsh, Can. J. Phys. 33, 588 (1965).

40. D. W. Lepard, D. M. C. Sweeney, and H. L. Welsh, Can. J. Phys. 40, 1567 (1962).

41. D. W. Lepard, D. E. Shaw, and H. L. Welsh, Can. J. Phys. 44, 2353 (1966).

42. D. E. Shaw and H. L. Welsh, Can. J. Phys. 45, 3823 (1967).

43. A. R. H. Cole, W. J. Lafferty, and R. J. Thiboult, J. Mol. Spectry. 29, 365 (1969).

44. J. Susskind, J. Mol. Spectry. 49, 1 (1974).

45. J. Susskind, J. Mol. Spectra. 49, 331 (1974).

46. R. N. Jones and T. Bach, Canada National Research Council, Bulletin No. 11 (1967).

47. T. Nakagawa and J. Overend, J. Mol. Spectry. 50, 333 (1974).

APPENDIXES

APPENDIX A

REPRODUCIBILITY OF THE LINE POSITIONS

When Part I of this project is undertaken, a synchronous motor is used to drive the scanning drive servo system in order that the drive screw rate remains as constant as possible throughout a spectral scan. Thus the value of $\frac{d\theta}{dx}$ for a particular scan can be written as

$$\frac{d\theta}{dx} = W + S(x) \tag{A.1}$$

where W is a constant and is the estimated constant value of $\frac{d\theta}{dx}$, and $S(x)$ represents the variation of $\frac{d\theta}{dx}$. Usually $S(x)$ can be considered to be a function that changes slowly in any given region of the spectrum. If $S(x)$ is so small that it is possible to reproduce $\theta(x)$ within the measurement error, then theoretically, it is possible to "calibrate the screw," i.e., determine $\theta(x)$ for the instrument. In most cases $S(x)$ is significant enough to affect the reproducibility of $\theta(x)$. The effect of $S(x)$ on the reproducibility of line positions can be derived as follows.

Let $\{x_1, x_2, \ldots, x_n\}$ be the measured line positions of a particular scan, which correspond to a set of θ-values, $\{\theta_1, \theta_2, \ldots, \theta_n\}$. If the scan is repeated, another set of measured line positions is determined. These are denoted by $\{y_1, y_2, \ldots, y_n\}$, and will correspond to the same set of θ-values, $\{\theta_1, \theta_2, \ldots, \theta_n\}$. If both x_1 and y_1 are set equal to 0, then

$$\theta_i - \theta_1 = \int_0^{x_i} (W_1 + S_1(x))\, dx \qquad (A.2)$$

for scan 1

and

$$\theta_i - \theta_1 = \int_0^{y_i} (W_2 + S_2(y))\, dy \qquad (A.3)$$

for scan 2

where W_1, W_2, $S_1(x)$, $S_2(y)$ stand for the values of W and S for scan 1 and scan 2, respectively.

It is useful to obtain an expression for $(x_i - y_i)$'s, since these values indicate the reproducibility of the scanning devices. Let the inverse function of $\theta(x)$ and $\theta(y)$ be defined by $x(\theta)$ and $y(\theta)$. This is possible because $\theta(x)$ and $\theta(y)$ are strictly monotonic functions. The value for $x_i - y_i$ can be expressed as follows,

$$x_i - y_i = x(\theta_i) - y(\theta_i) = \int_{\theta_1}^{\theta_i} \left(\frac{dx}{d\theta} - \frac{dy}{d\theta}\right) d\theta$$

$$= \int_{\theta_1}^{\theta_i} \left(\frac{1}{\frac{d\theta}{dx}} - \frac{1}{\frac{d\theta}{dy}}\right) d\theta$$

$$= \int_{\theta_1}^{\theta_i} \frac{\left(\frac{d\theta}{dy} - \frac{d\theta}{dx}\right)}{\frac{d\theta}{dx} \cdot \frac{d\theta}{dy}}\, dz \; . \qquad (A.4)$$

Usually $\frac{d\theta}{dx} \approx \frac{d\theta}{dy}$ so the last expression can be simplified by setting $\frac{d\theta}{dx} = \frac{d\theta}{dy}$ in the denominator and obtaining

$$x_i - y_i = \int_{\theta_1}^{\theta_i} \frac{(\frac{d\theta}{dy} - \frac{d\theta}{dx})}{(\frac{d\theta}{dx})^2} dz \ . \qquad (A.5)$$

From Eq. (A.5) it is clear that the values for $(x_i - y_i)$'s are roughly proportional to the accumulated difference of $\frac{d\theta}{dx}$ and $\frac{d\theta}{dy}$.

In the special case that the values for $\frac{d\theta}{dx} - \frac{d\theta}{dy}$ are randomly distributed, the expectation values of $x_i - y_i$ can be derived from "random walk theory" (4,5).

Let the variance of $\frac{d\theta}{dx} - \frac{d\theta}{dy}$ be denoted by σ^2. If the expectation value of $(s_i - t_i)^2$ is denoted by Σ_i^2, then from Eq. (A.5) and random walk theory, the value of Σ_i^2 can be obtained as

$$\Sigma_i^2 \approx \sigma^2 \cdot (\theta_i - \theta_1)/(\frac{d\theta}{dx})_{av}^2$$

$$\approx \sigma^2 \cdot (s_i - \ _1)/(\frac{d\theta}{dx})_{av} \ . \qquad (A.6)$$

The last expression implies that the difference between s_i and t_i will tend to increase as the values for s_i and t_i become larger.

APPENDIX B

APPLICATION OF THE AVERAGE LINE POSITIONS IN THE CALIBRATION OF SPECTRA

When there are several scans of the same spectra, one usually fits each spectrum separately to Eq. (1.5) and takes the average of the separately determined wavenumbers for each line as experimental results (this will be called method A). It will be shown that better results can be obtained if we average the data scale and fit Eq. (1.5) only once (this will be called method B).

The validity of method B will be demonstrated for two scans. It can be easily extended to an arbitrary number of scans. The calibration polynomial for each spectrum is:

$$\text{(i)} \quad \hat{\nu}_{i1} = \sum_{k=0}^{m} a_{k1} x_{i1}^{k} \quad \ldots \text{ for scan 1} \tag{B.1}$$

$$\text{(ii)} \quad \hat{\nu}_{i2} = \sum_{k=0}^{m} a_{k2} x_{k2}^{k} \quad \ldots \text{ for scan 2 .} \tag{B.2}$$

($\hat{\nu}_i$ is the predicted frequency in cm^{-1} of the standard line, and k, m are integers.) There is a strict one-to-one relation between $\hat{\nu}_i$ and x_{ij}. So we can write, by reversion of series,

$$\hat{x}_{i1} = \sum_{k=0}^{m} b_{k1} \nu_{i1}^{k} \tag{B.3}$$

$$\hat{x}_{i2} = \sum_{k=0}^{n} b_{k2} \nu_{i2}^{k} \tag{B.4}$$

where $\nu_{i\ell}$ is the standard frequency in cm^{-1} of the standard line and $\hat{x}_{i\ell}$ is the predicted value of x for a given $\nu_{i\ell}$. (Empirically, $n \approx m$.) Since $\nu_{i1} = \nu_{i2} - \nu_i$, adding Eqs. (B.3) and (B.4), and halving, we obtain

$$\frac{1}{2} (\hat{x}_{i1} + \hat{x}_{i2}) = \sum_{k=0}^{m} \frac{1}{2} (b_{k1} + b_{k2}) \nu_i^k \ . \tag{B.5}$$

Letting

$$\frac{1}{2} (\hat{x}_{i1} + \hat{x}_{i2}) = \hat{x}_{i,av} \tag{B.6}$$

and defining

$$\Delta x_{i1} = x_{i1} - \hat{x}_{i1} \tag{B.7}$$

$$\Delta x_{i2} = x_{i2} - \hat{x}_{i2} \tag{B.8}$$

we can obtain

$$\frac{1}{2} (\Delta x_{i1} + \Delta x_{i2}) = \frac{1}{2} (x_{i1} + x_{i2}) - \frac{1}{2} (\hat{x}_{i1} + \hat{x}_{i2})$$

$$= \frac{1}{2} (x_{i1} + x_{i2}) - \hat{x}_{i,av} \ .$$

The standard deviation for Eq. (B.5) is estimated by $\hat{\Sigma}$ = [expectation value of

$$\left[\frac{1}{4}\,(\Delta x_i + \Delta x_i)^2\right]^{1/2}$$

$$= \left(\frac{1}{4}\,\overline{(\Delta x_{i1} + \Delta x_{i2})^2}\right)^{1/2}$$

$$= \left(\frac{1}{4}\,\overline{(\Delta x_{i1})^2 + 2(\Delta x_{i1} \cdot \Delta x_{i2}) + (\Delta x_{i2})^2}\right)^{1/2} .$$

Since Δx_{i1} and Δx_{i2} are uncorrelated, then $\overline{\Sigma x_{i1} \cdot \Sigma x_{i2}} = 0$. It is then possible to write

$$\hat{\Sigma} = \frac{1}{2}\,(\sigma_1^2 + \sigma_2^2)$$

$$\cong \frac{\sigma}{\sqrt{2}} \cdot (\sigma_1 \simeq \sigma_2 \approx \sigma) . \qquad \text{(B.9)}$$

Thus $\sigma/\sqrt{2}$ is an upper bound of the standard deviation for a new and obviously improved least square fit; i.e.,

$$\hat{x}_{i,av} = \Sigma C_k\, \nu_i^k .$$

Likewise, a smaller standard deviation can be expected for the normal calibration fit

$$\hat{\nu}_i = \Sigma\, d_k\, x_{i,av} .$$

VITA

K. Frank Lin was born in Huwei, Taiwan, on May 7, 1948. He attended public school in Huwei. He studied at Provincial Huwei High School for four years. Then he transferred to City Chien-Kuo High School. He entered National Tsing-Hua University in 1966 and received a Bachelor of Science degree in Physics in May, 1970.

In 1971, he came to study at the University of Tennessee. He received a Master of Science degree in Physics in March, 1973. He began his research at the University of Tennessee Molecular Spectroscopy Laboratory in June, 1973. He received the Doctor of Philosophy degree in Physics in March, 1977.

He is a member of Sigma Pi Sigma and Phi Kappa Phi.

He married B. Sherry Huang in Huwei in August, 1971.